X-ray Wakefield Accelerator on a Chip

LLNL HEDS Center
Livermore, CA
April 27, 2017

Toshiki Tajima

Norman Rostoker Chair Professor, UC Irvine

Acknowledgements: G. Mourou, J. A. Wheeler, X. M. Zhang, D. Farinella, F. Dollar, T. Nguyen, S. Mironov, S. Hakimi , K. Nakajima, Y.M. Shin, M. Zhou, X. Q. Yan, P. Taborek

abstract

New technology thin film compression (TFC) [and coherent amplification network (CAN)] → Leading to a new innovation X-ray LWFA (and single-cycled laser acceleration of ions)

1. **Introduction to wakefield, relativistic coherence, and Tsunami**
2. **Toward high reprate and high efficiency fiber laser (CAN)**
3. **Single-cycled laser by TFC (Thin Film Compression) and further compression by relativistic compression**
4. **“TeV on a chip” (X-ray LWFA); coherent γ-ray laser, zeptosecond science**
5. **Compact ion acceleration (short-lived isotope generation, ADS)**

Introduction to Wakefield

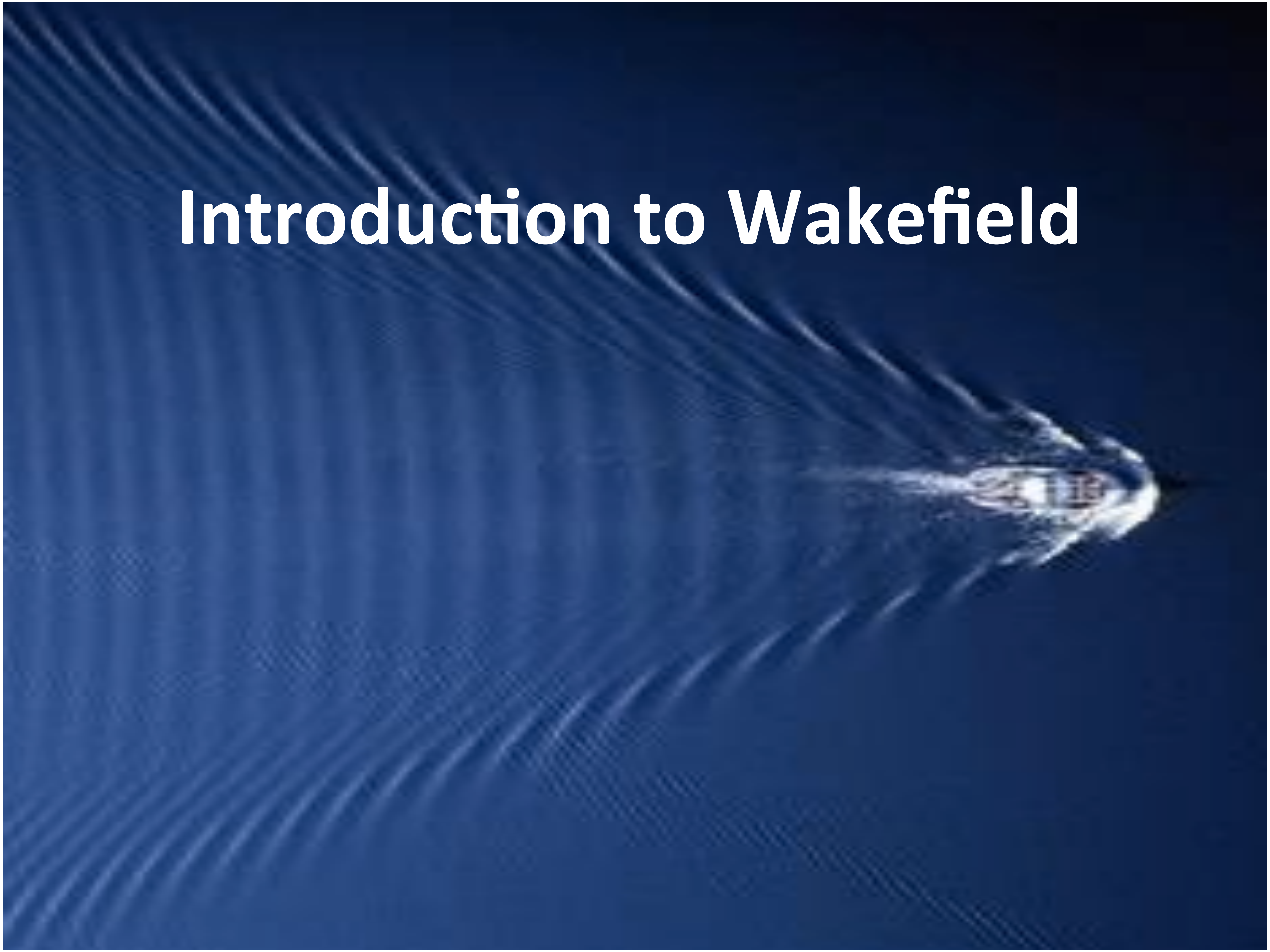

Laser Wakefield (LWFA):

Wake phase velocity >> water movement speed
maintains **coherent** and **smooth** structure

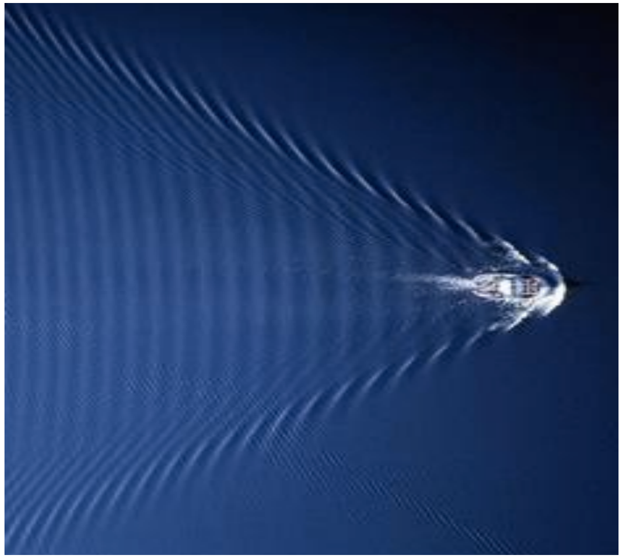

vs

Tsunami phase velocity becomes ~0,
causes **wavebreak** and **turbulence**

Strong beam (of laser / particles) drives plasma waves to saturation amplitude: $E = m\omega v_{ph}/e$

No wave breaks and wake **peaks** at v≈c

Wave **breaks** at v<c

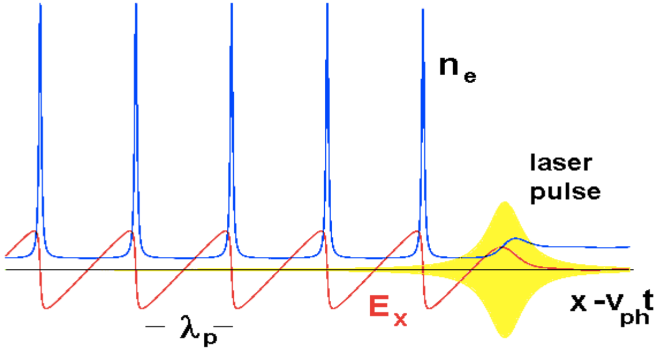

← relativity regularizes
(***relativistic coherence***)

Relativistic coherence enhances beyond the Tajima-Dawson field $E = m\omega_p c/e$ (~ GeV/cm)

Wakefields and Higgs

Laundau-Ginzburg potential → BCS → Nambu → Higgs vacuum

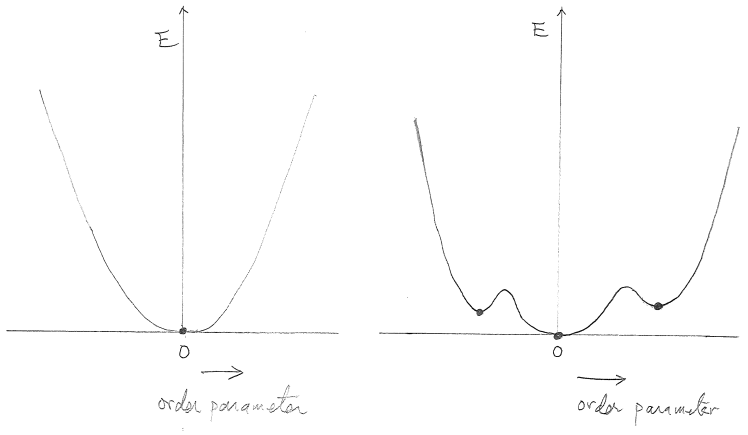

Landau damping: decay of excited waves to equilibrium (left picture)

Wakefield: no damping; distinct excited stable state ←no particles to resonate (@ c)

= plasma's elevated Higgs state

| 0 > vs. | H > (cf . | H > → | 0 >)

thermo-equilibrium wakefield state tsunami onshore

Theory of wakefield toward extreme energy

$$\Delta E \approx 2m_0c^2a_0^2\gamma_{ph}^2 = 2m_0c^2a_0^2\left(\frac{n_{cr}}{n_e}\right),$$ (when 1D theory applies)

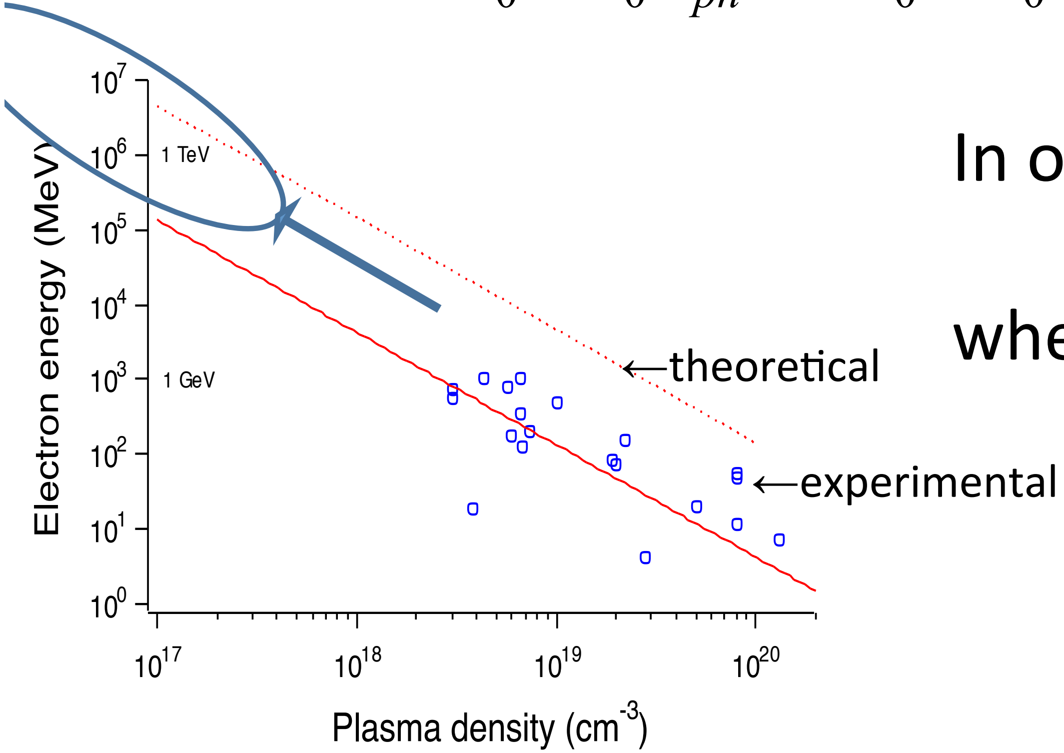

In order to avoid wavebreak,

$$a_0 < \gamma_{ph}^{1/2},$$

where

$$\gamma_{ph} = (n_{cr} / n_e)^{1/2}$$

$n_{cr} = 10^{21}$

$n_e = 10^{16}$

$$L_d = \frac{2}{\pi}\lambda_p a_0^2\left(\frac{n_{cr}}{n_e}\right),$$

dephasing length

$$L_p = \frac{1}{3\pi}\lambda_p a_0\left(\frac{n_{cr}}{n_e}\right),$$

pump depletion length

LWFA and CAN laser

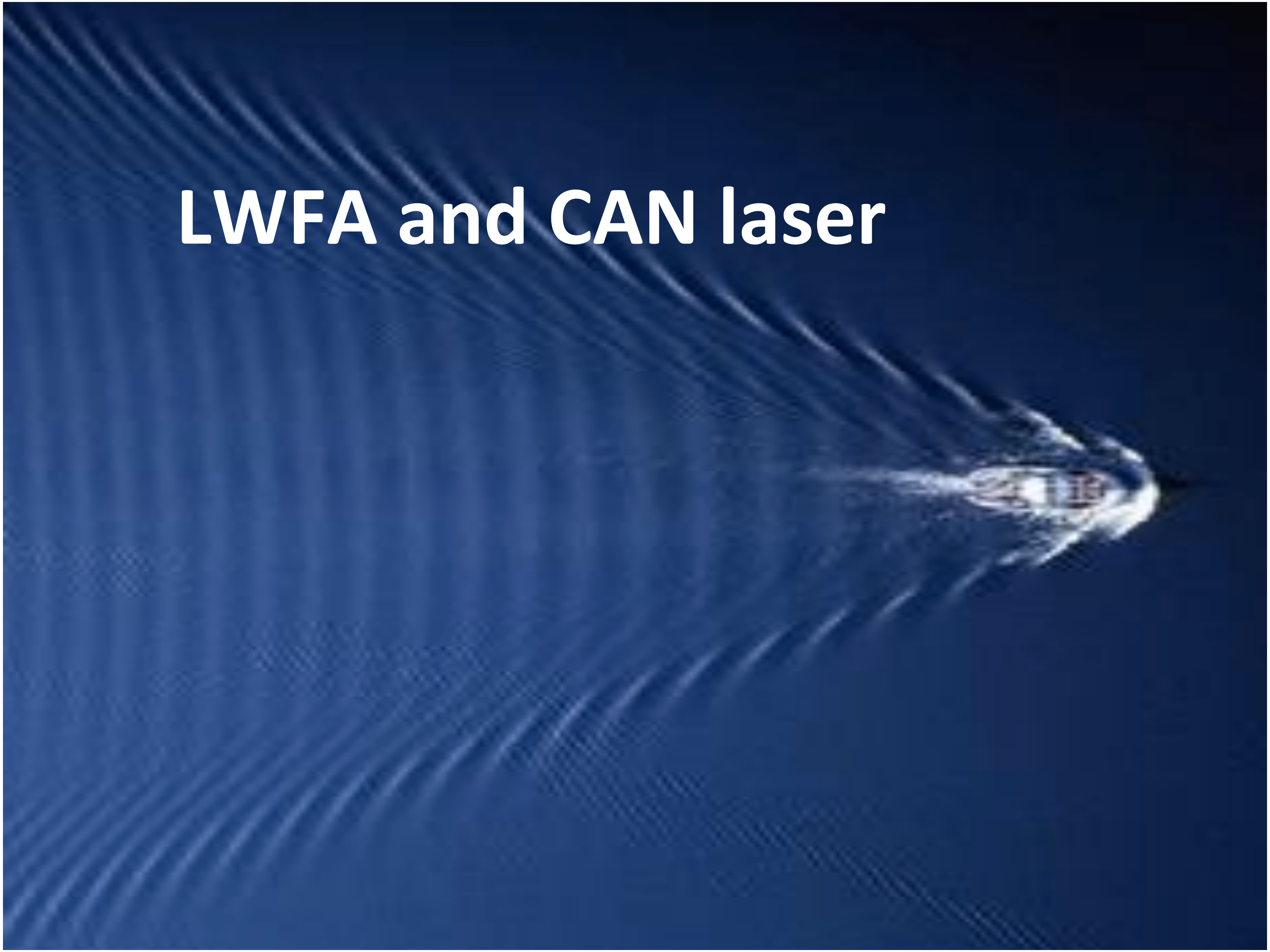

Energy gain VS Plasma density

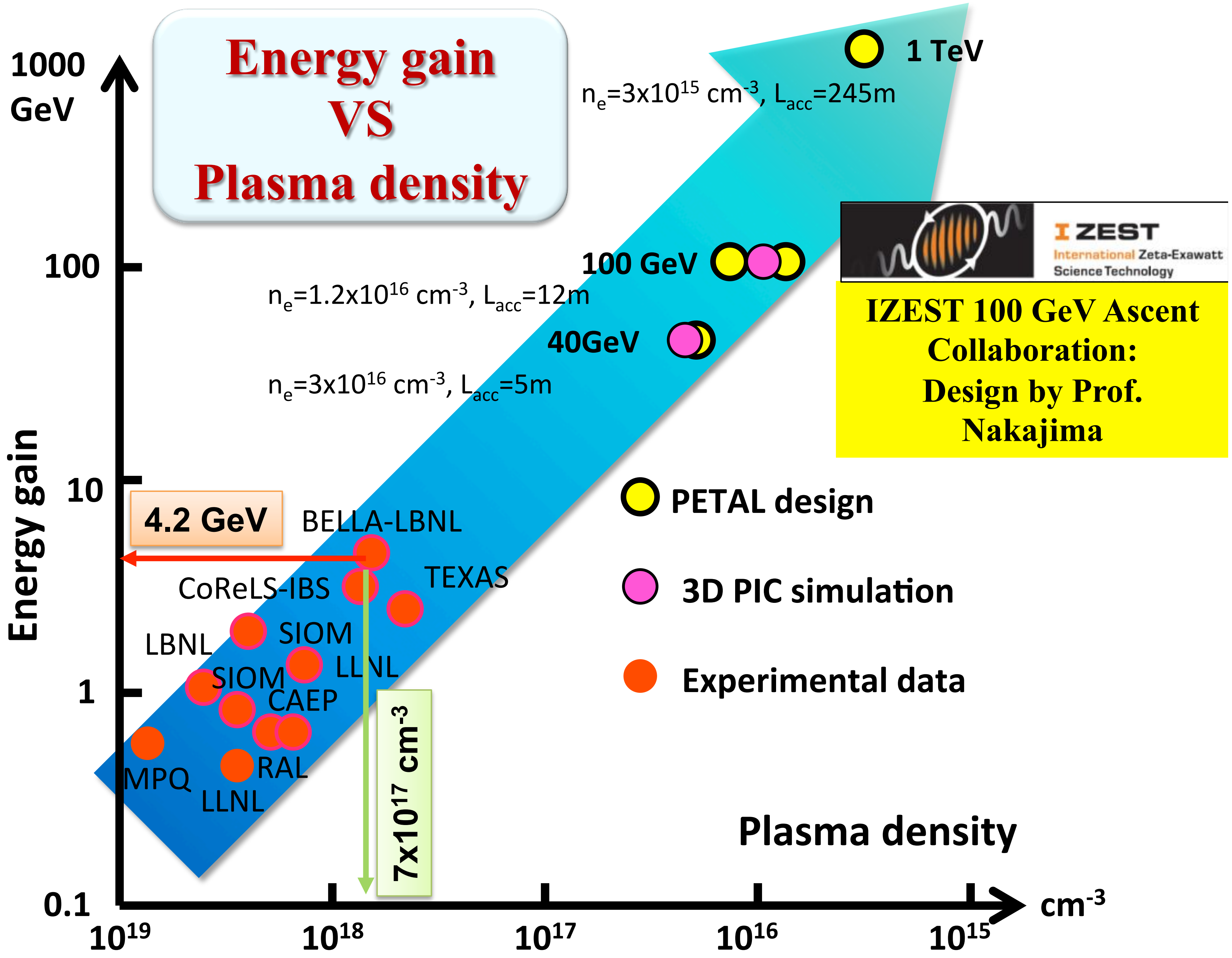

IZEST 100 GeV Ascent Collaboration: Design by Prof. Nakajima

Method 1

Ablative Discharge Plasma Waveguide-Meter Module

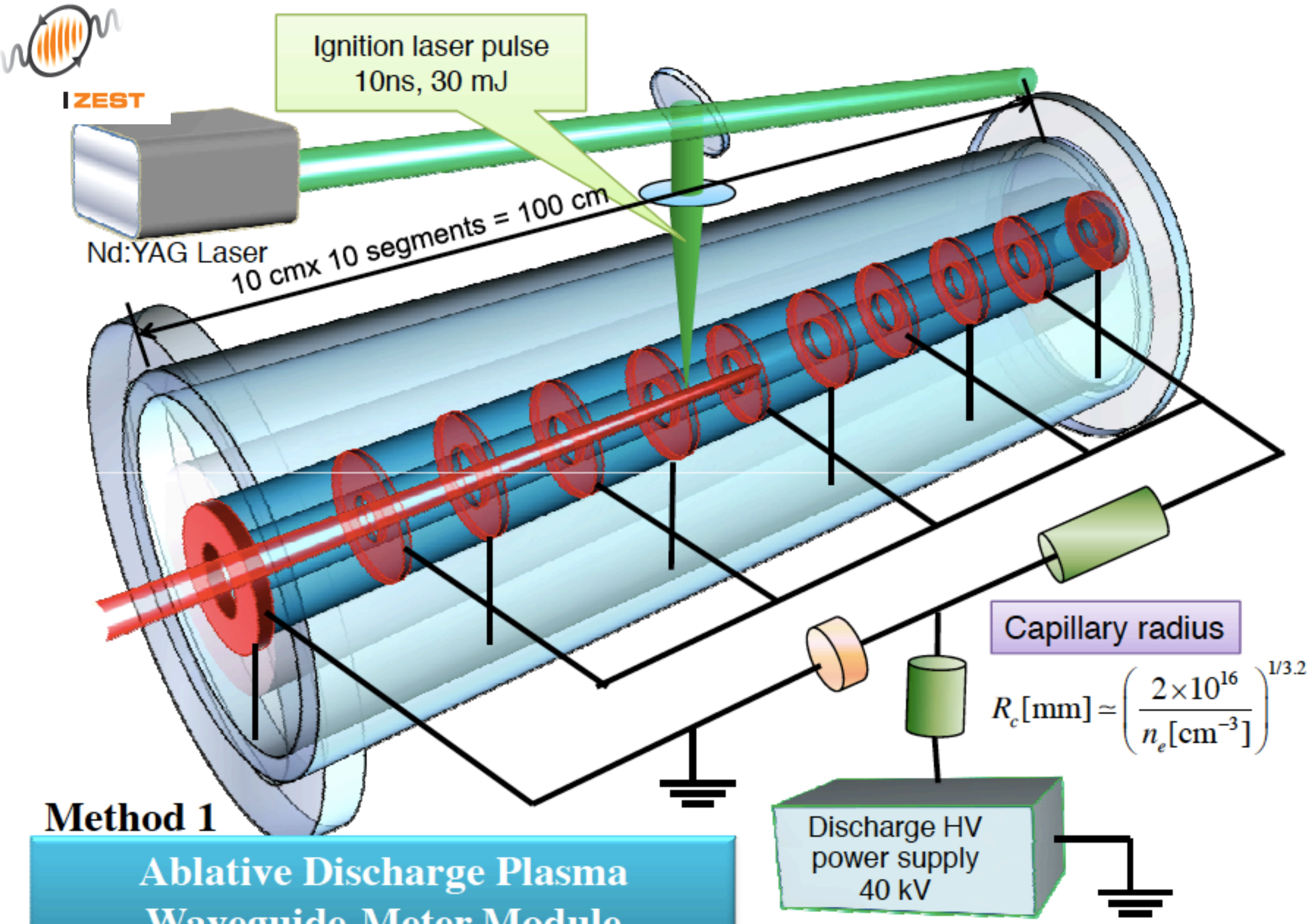

Capillary radius

$$R_c[\text{mm}] \simeq \left(\frac{2\times10^{16}}{n_e[\text{cm}^{-3}]}\right)^{1/3.2}$$

Nakajima, 2016

Areas of improvement in LA performance for various applications

(from Darmstadt JTF workshop, 2010; also in Final Report of JTF: W. Leemans, W. Chou, M. Uesaka)

	THz	X-rays (betatron)	FEL (XUV)	Gamma-rays	FEL (X-rays)	Collider
Energy	✓	✓	✓	✓	↑	↑↑
ΔE/E	✓	✓	↓	↓	↓↓	↓↓
ε	✓	✓	✓	✓	✓	↓↓
Charge	✓	✓	✓	↑	✓	↑
Bunch duration	✓	✓	✓	✓	✓	✓
Avg. power	↑	↑	↑	↑	↑	↑↑

✓: OK as is
↑: increase needed
↓: decrease needed

Coherent Amplification Network

Need to Phase

32 J/1mJ/fiber~ 3x10^4 Phased Fibers!

<u>High rep-rated</u>, <u>efficient</u>, <u>digital control</u> possible

Mourou, Brocklesby, Tajima, Limpert,
Nature Photonics (2013)

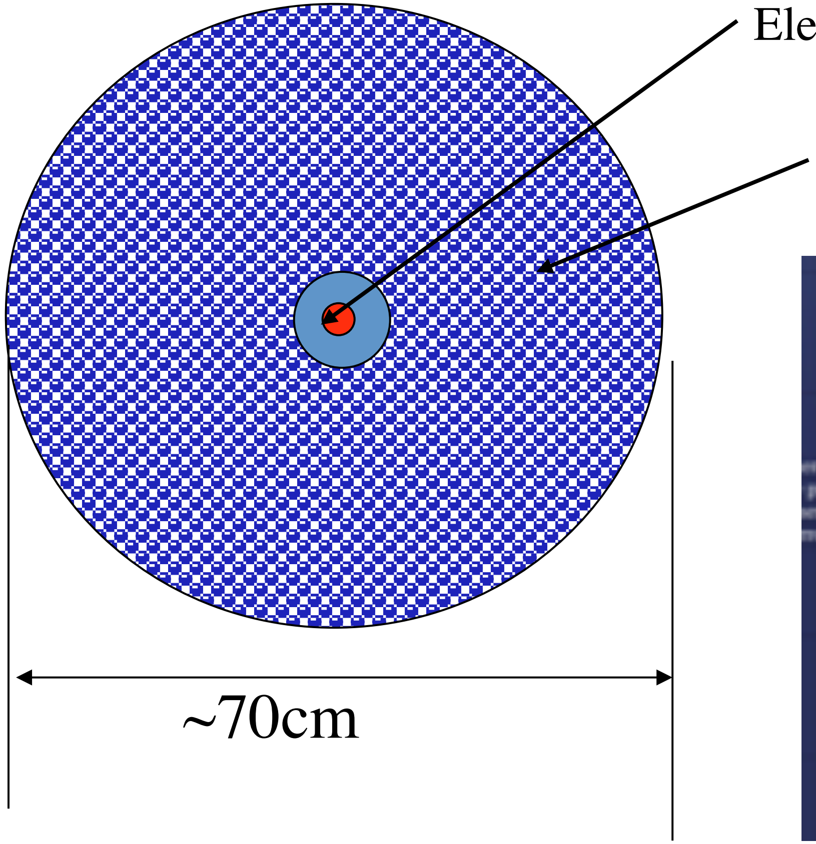

Electron/positron beam

Transport fibers

~70cm

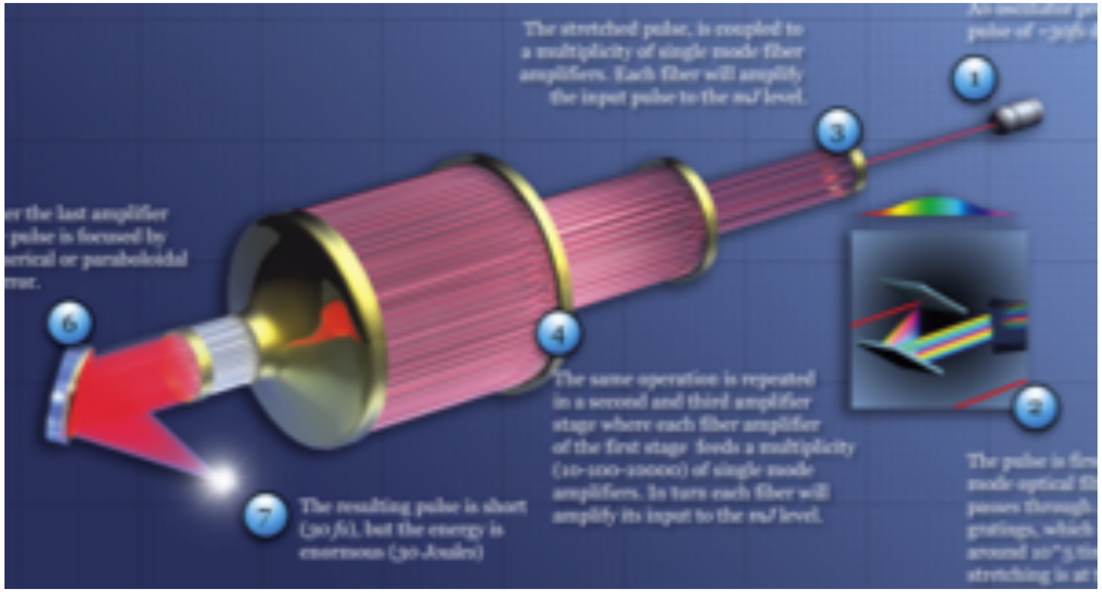

The stretched pulse, is coupled to a multiplicity of single mode fiber amplifiers. Each fiber will amplify the input pulse to the mJ level.

er the last amplifier
pulse is focused by
erical or paraboloidal
rror.

The same operation is repeated in a second and third amplifier stage where each fiber amplifier of the first stage feeds a multiplicity (10-100-10000) of single mode amplifiers. In turn each fiber will amplify its input to the mJ level.

The resulting pulse is short (30 fs), but the energy is enormous (30 Joules)

Length of a fiber ~2m   Total fiber length~ 5 10^4km

J. Bourderionnet, A. Brignon (Thales), C. Bellanger, J. Primot (ONERA)

Coherent Fiber Combining

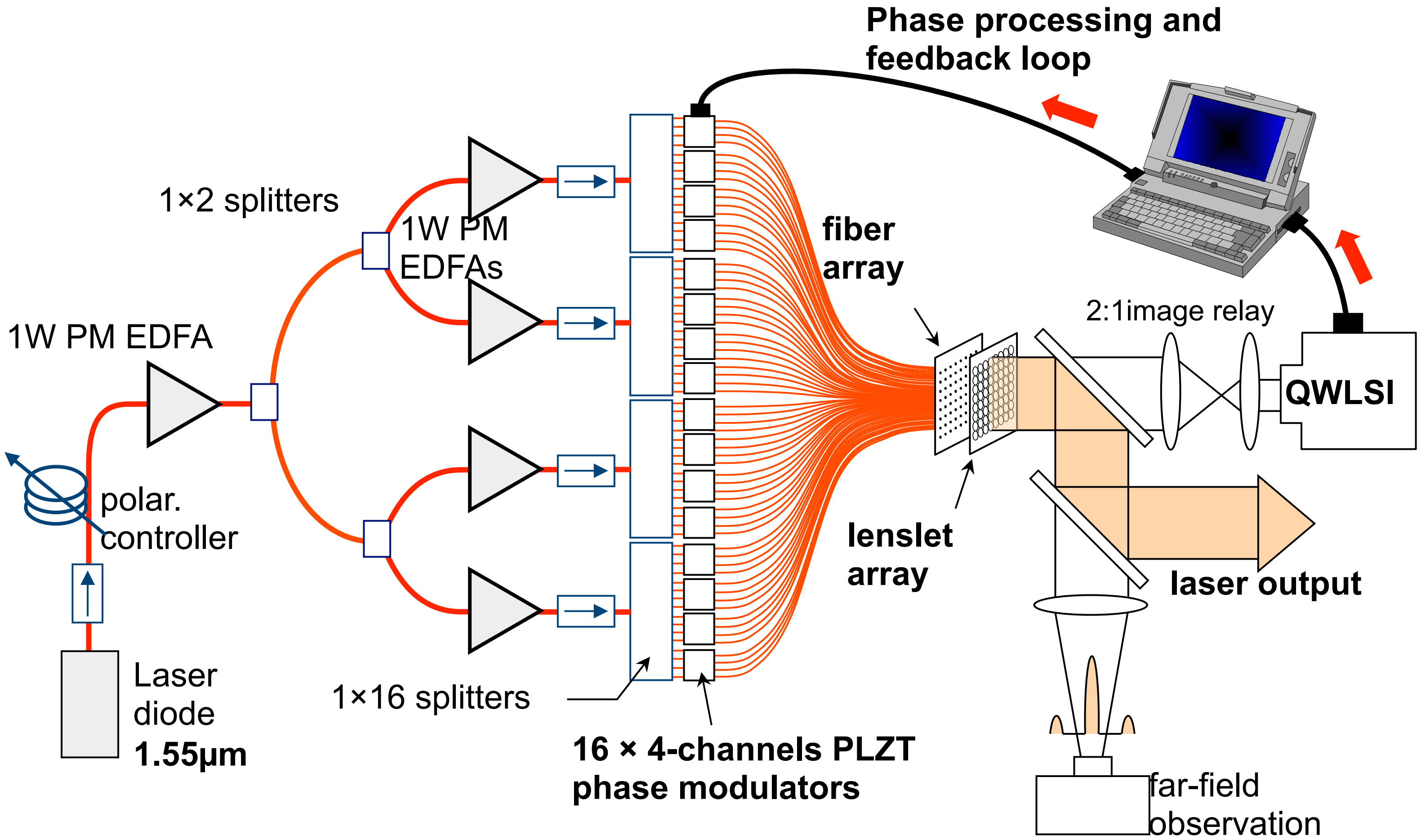

Achievement 2011
→ 64 phase-locked fibers

→ XCAN project

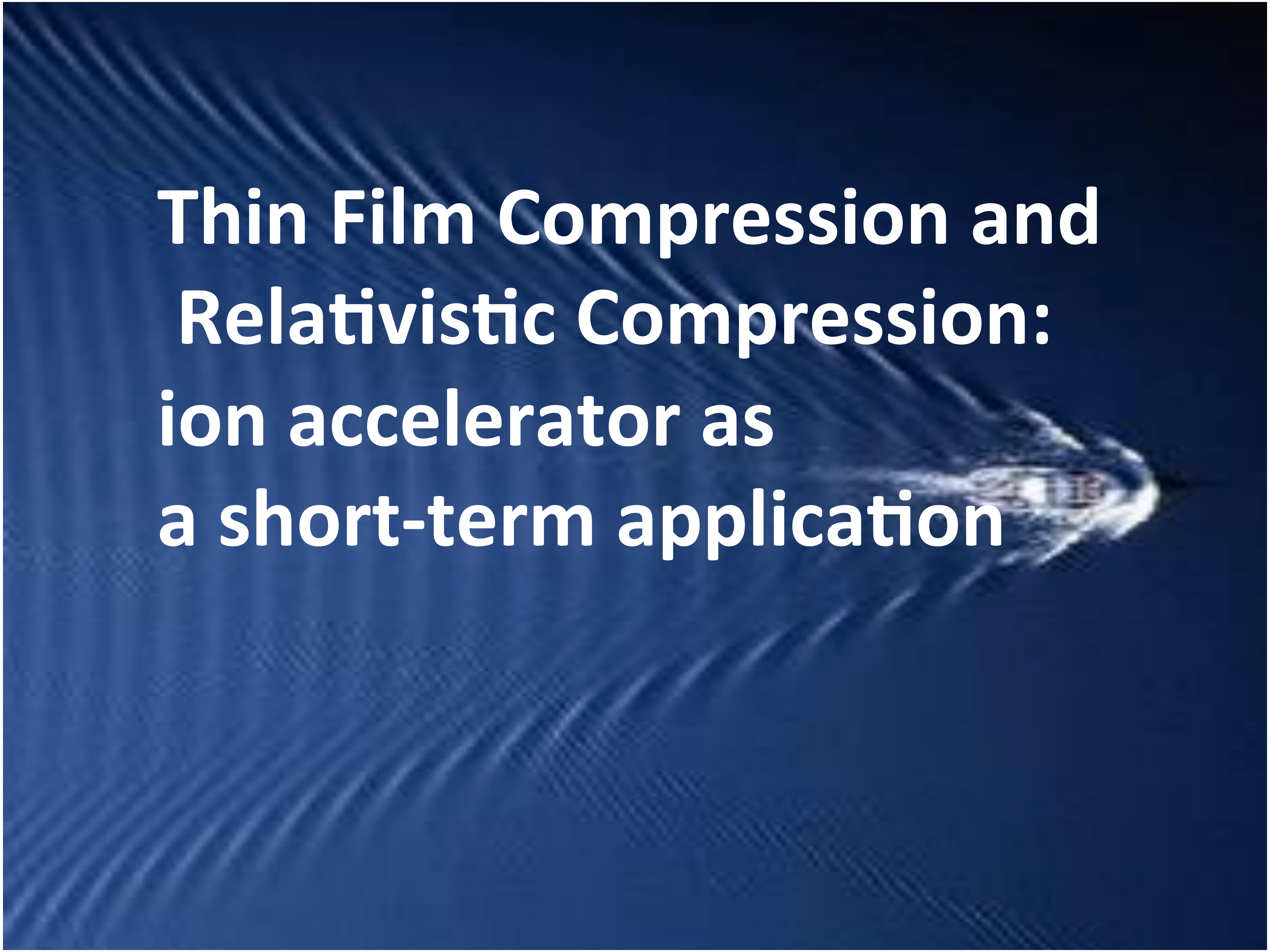

Thin Film Compression and Relativistic Compression: ion accelerator as a short-term application

Single-cycle laser (new Thin Film Compression)

Laser power = energy / pulse lnegth

Optical nonlinearity of thin film → pulse frequency width bulge, pulse compression

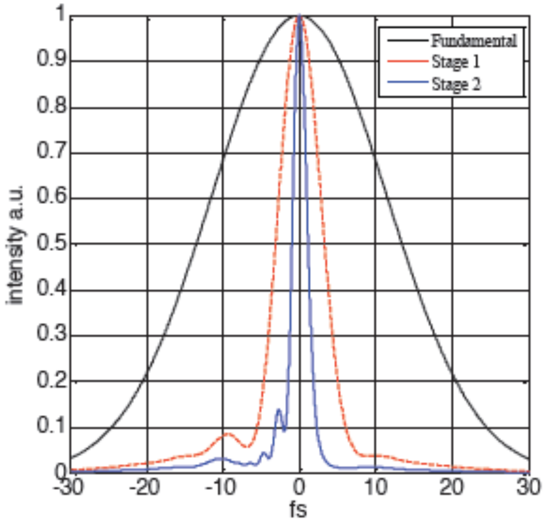

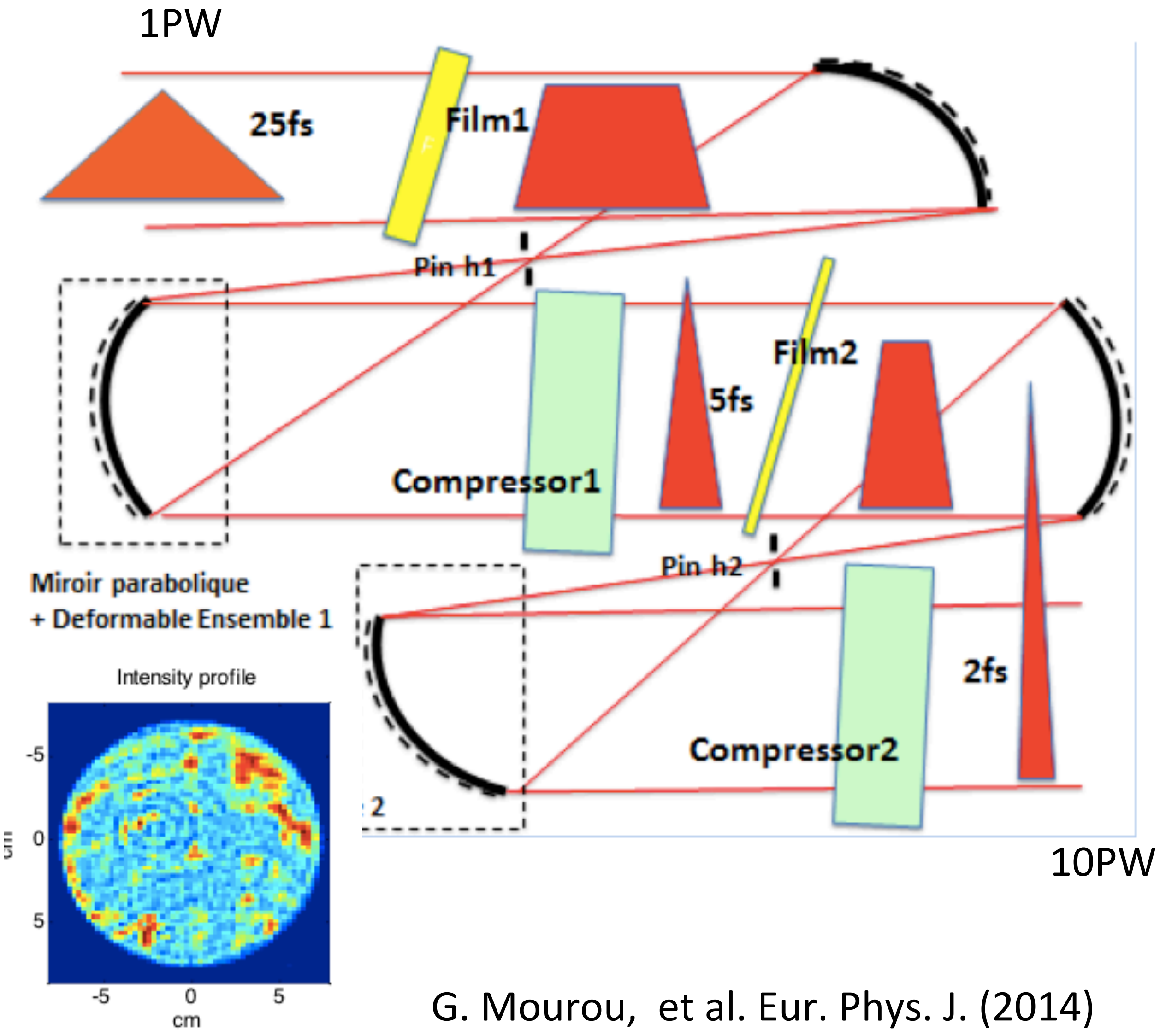

G. Mourou, et al. Eur. Phys. J. (2014)

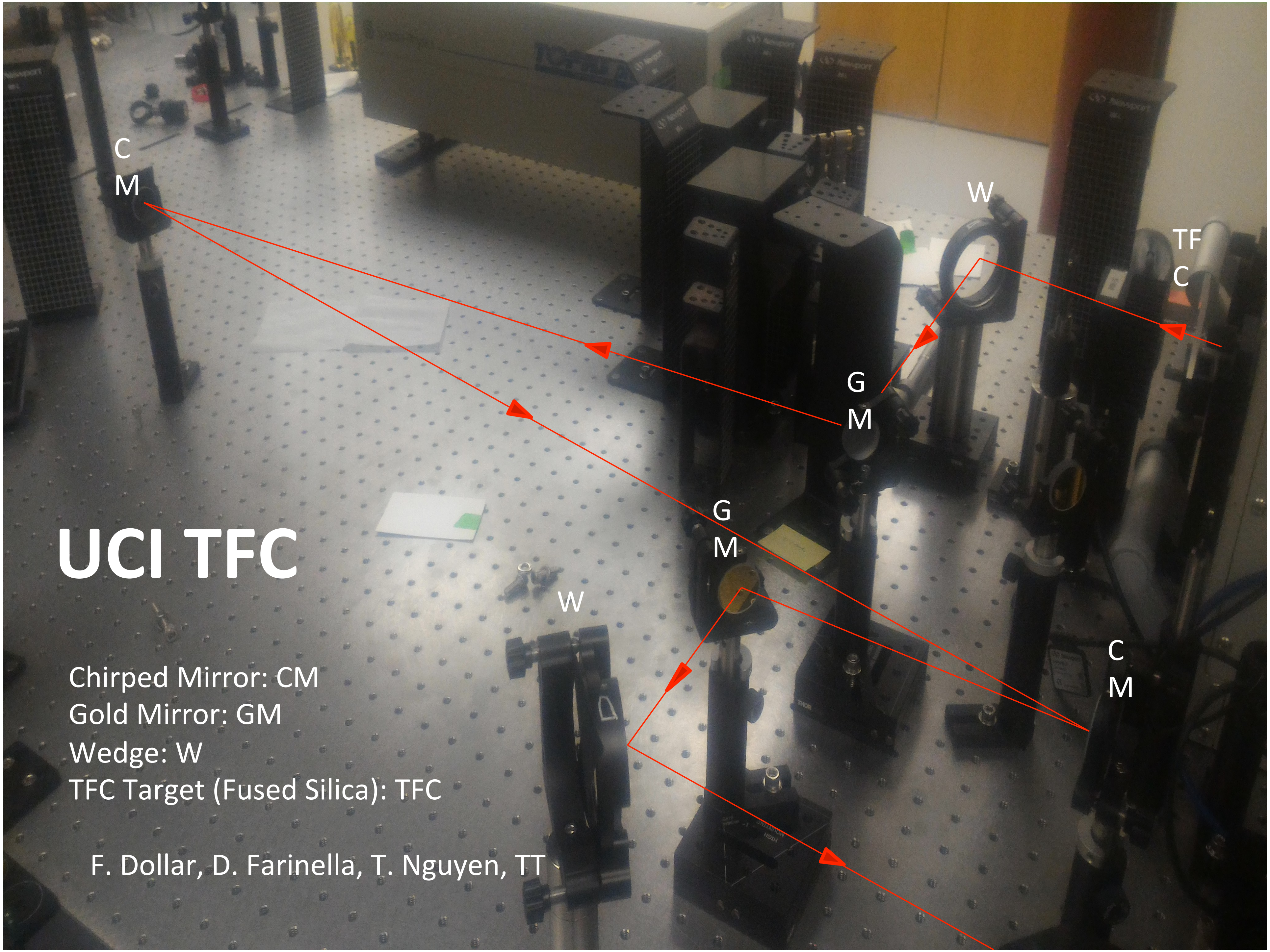

UCI TFC

Chirped Mirror: CM
Gold Mirror: GM
Wedge: W
TFC Target (Fused Silica): TFC

F. Dollar, D. Farinella, T. Nguyen, TT

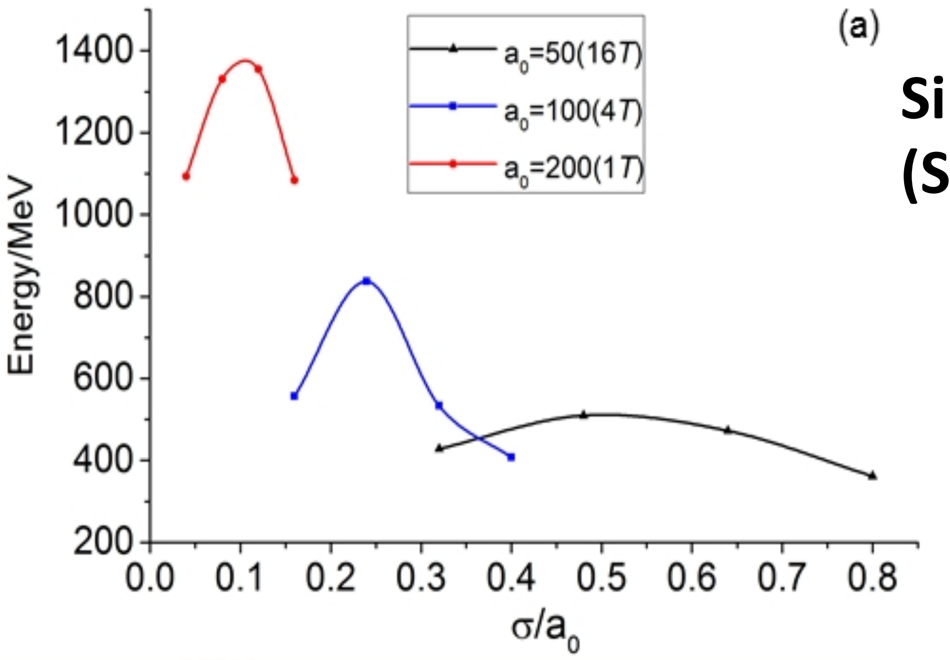

Single-Cycled **Laser** Acceleration (SCLA)

more coherent acceleration under same laser energy: more energies proportional to a_0

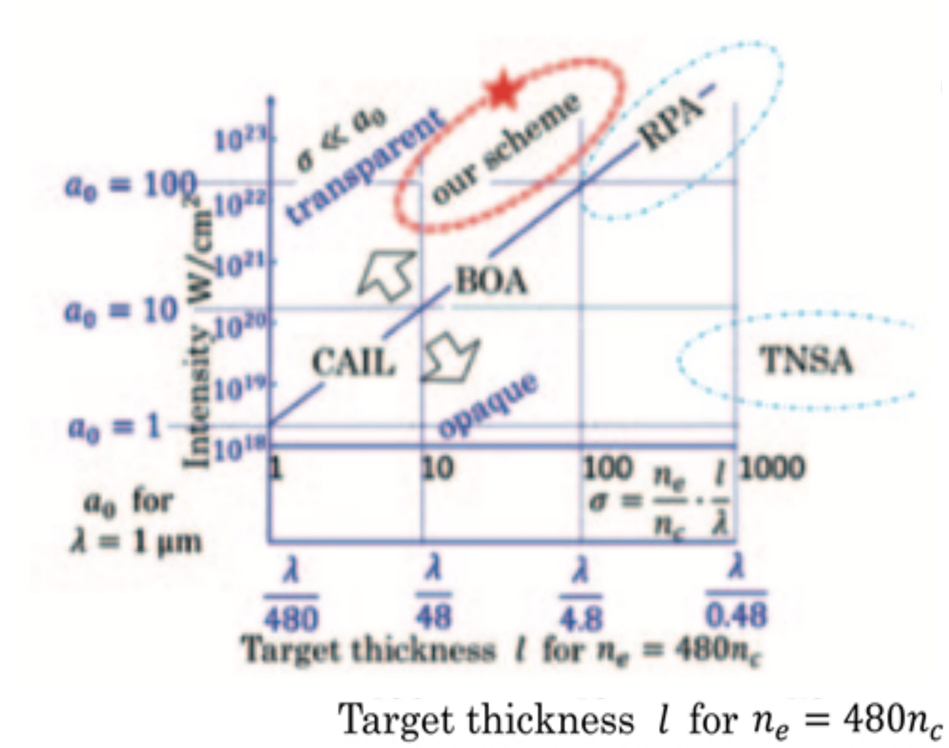

Domain map of various ion accelerations in a_0 and σ

Zhou et al. PoP (2016)

Thin Film Compression (TFC) into a Single-Cycled Laser Pulse

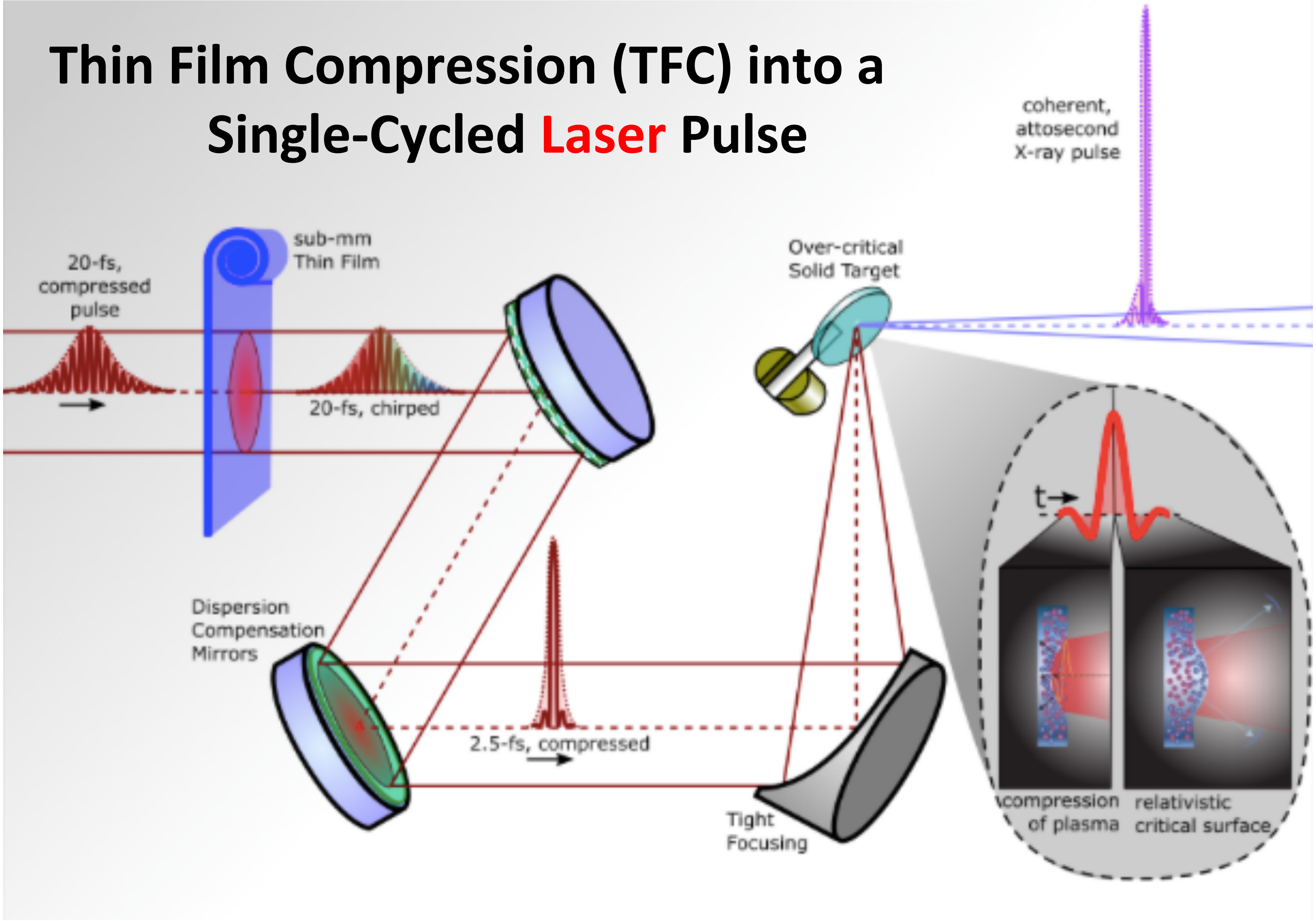

Mourou et al. (2014)

Ultrarelativistic Mirror in the λ^3 -laser Regime

(second step)

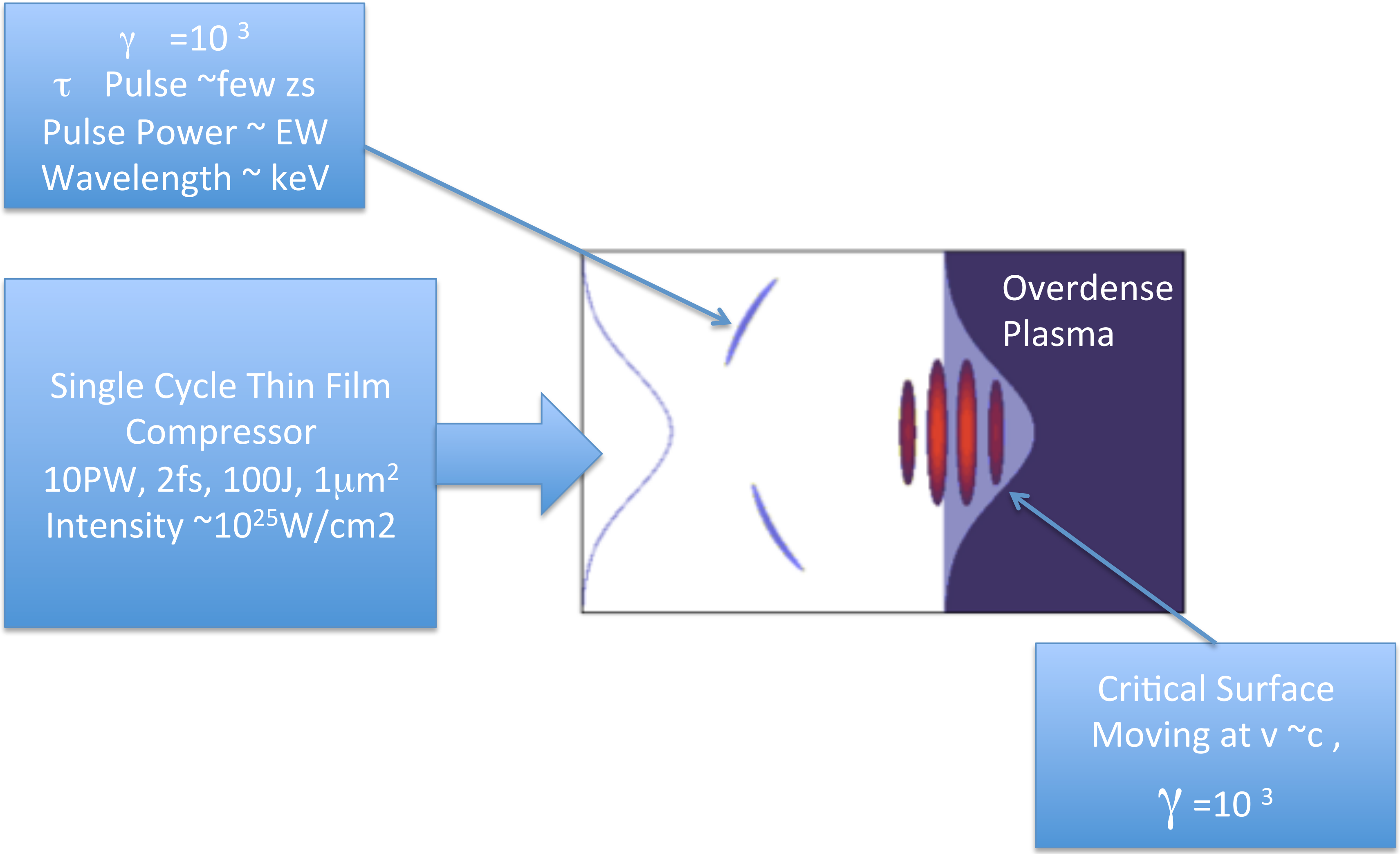

γ $=10^3$
τ Pulse ~few zs
Pulse Power ~ EW
Wavelength ~ keV

Single Cycle Thin Film Compressor
10PW, 2fs, 100J, 1μm^2
Intensity ~10^{25}W/cm2

Critical Surface Moving at v ~c ,
γ $=10^3$

N. M. Naumova, et al. Phys. Rev. Lett. (2004).

Relativistic Compression

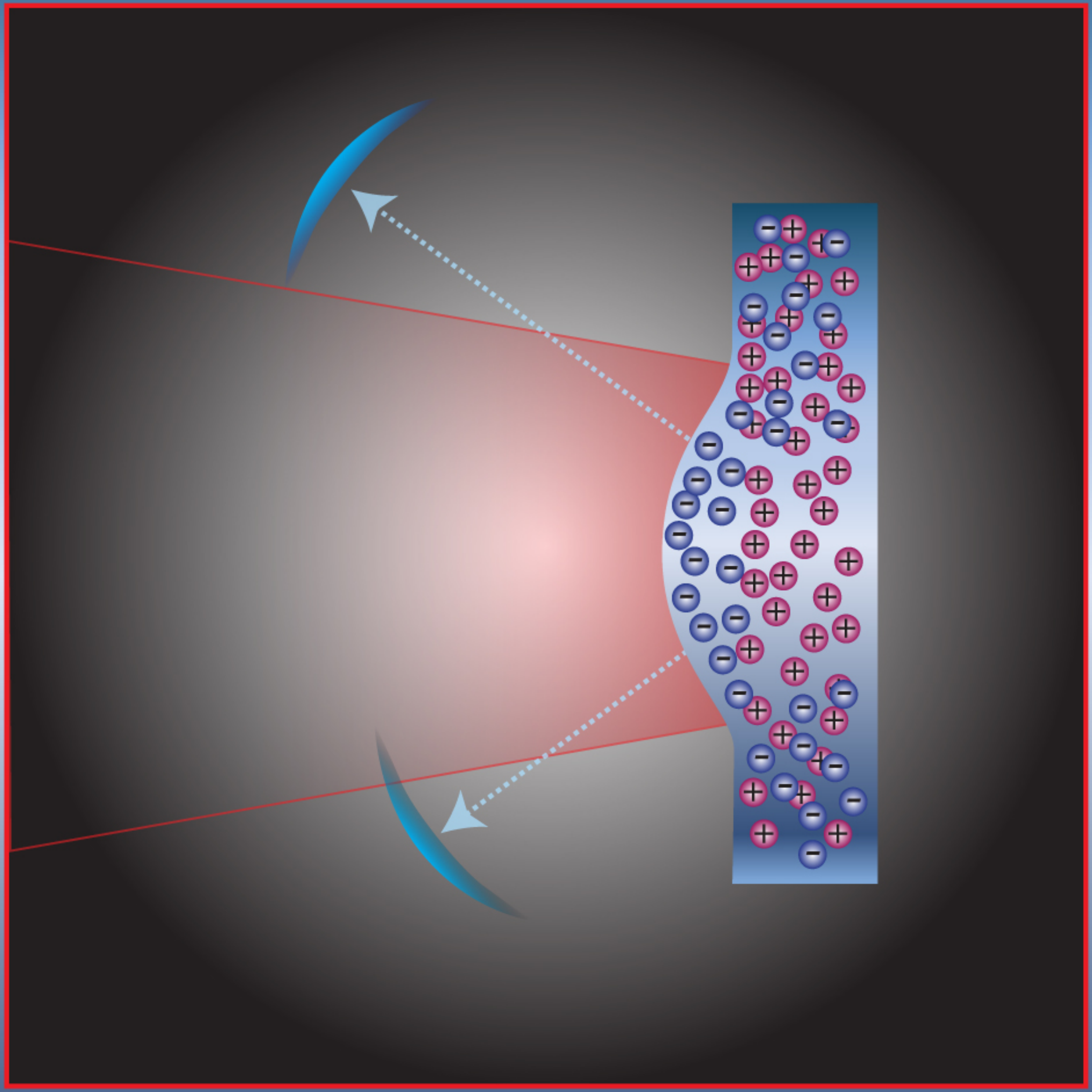

Even,isolated zeptosecond X-ray laser pulse possible

(simulation by N. Naumova, et al., 2014)

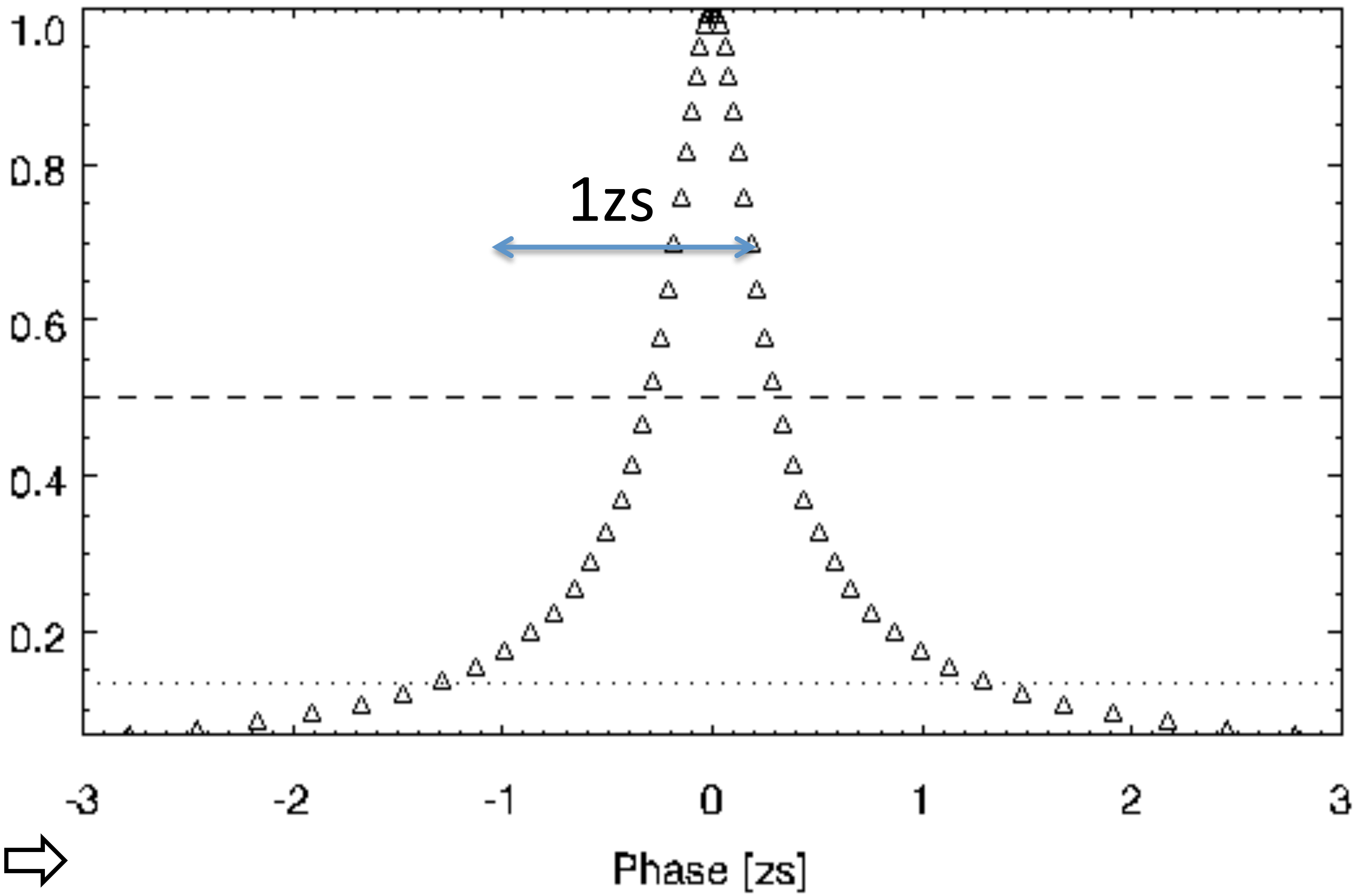

⇨

1PW optical laser → 10PW single osc. Optical laser

→ EW single osc. X-ray laser

Consistent with “Intensity-pulse-width Conjecture” (Mourou-Tajima, Science **331** (2011))

Petawatt laser / secondary rays vs SR, XFEL, and SCXL

Brilliance of our Single Cycled X-ray Laser (SCXL)

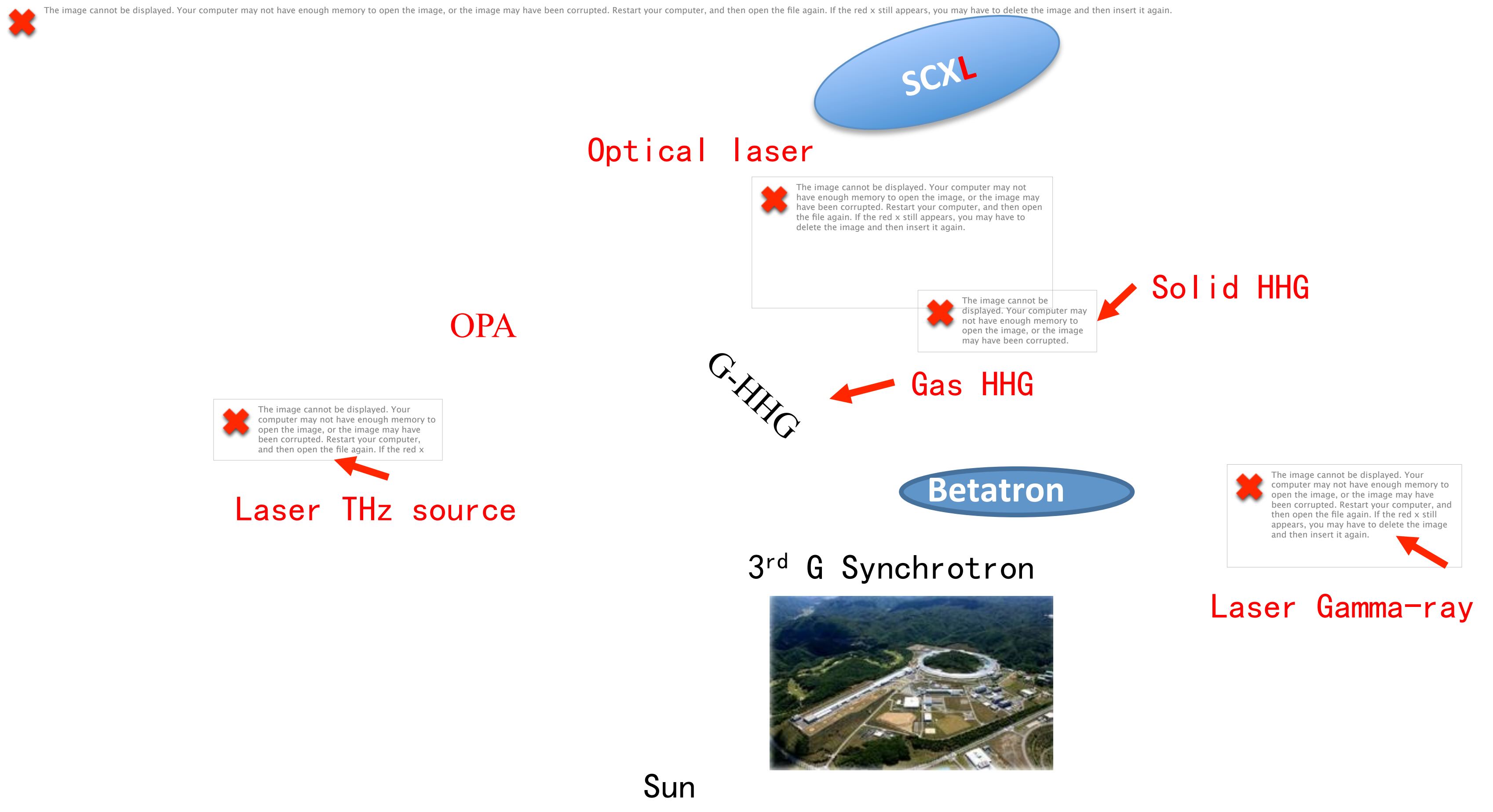

SCXL added to T.J. Wang / R. X. Li (2016)

X-ray LWFA in Nanostructure

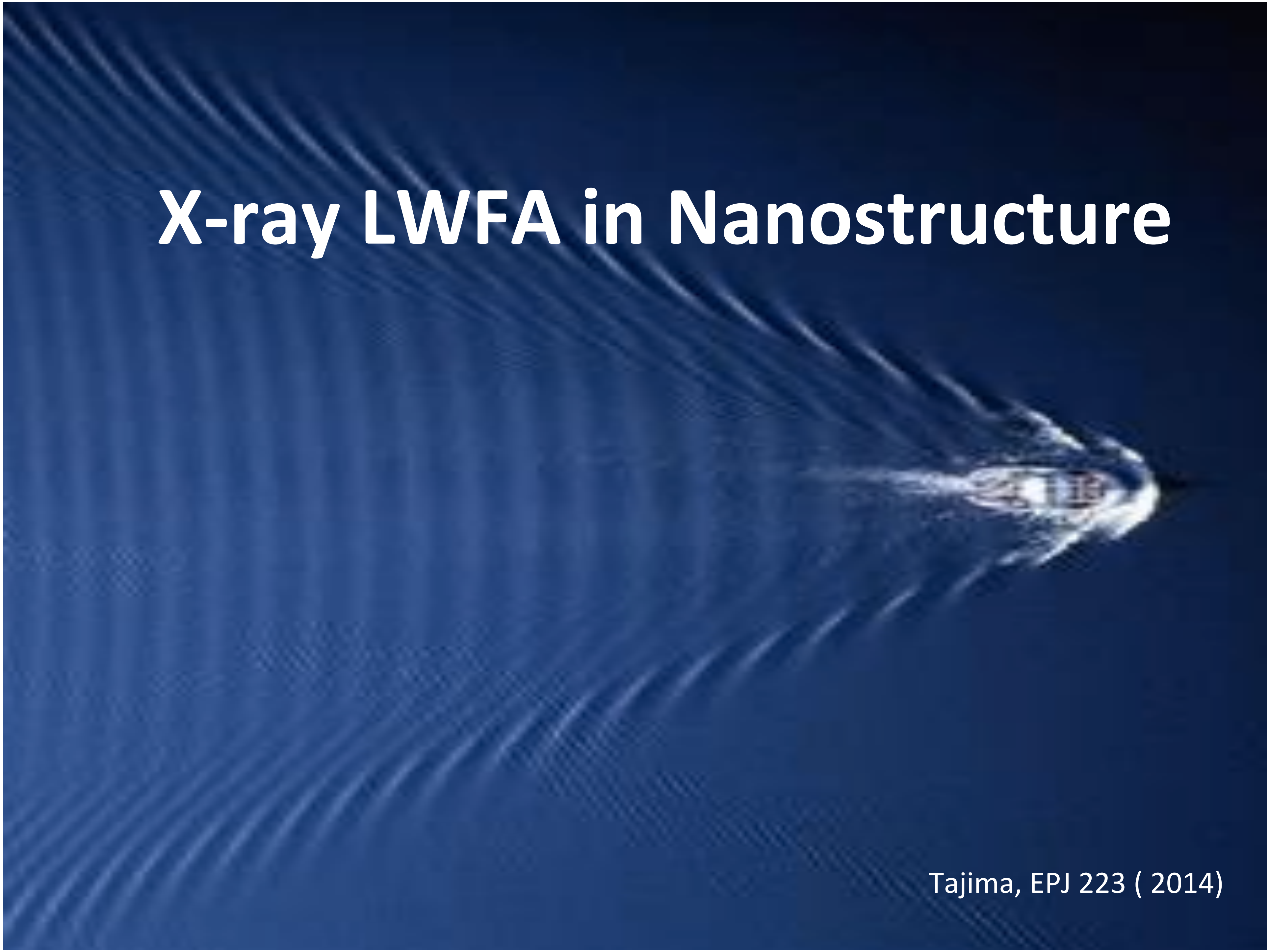

Tajima, EPJ 223 (2014)

Earlier works of X-ray crystal acceleration

-X-ray optics and fields (Tajima et al. PRL,1987)

-**Nanocrystal hole** for particle propagation (Newberger, Tajima, et al. 1989, AAC; PR,..)

-particle transport in the crystal (Tajima et al. 1990, PA)

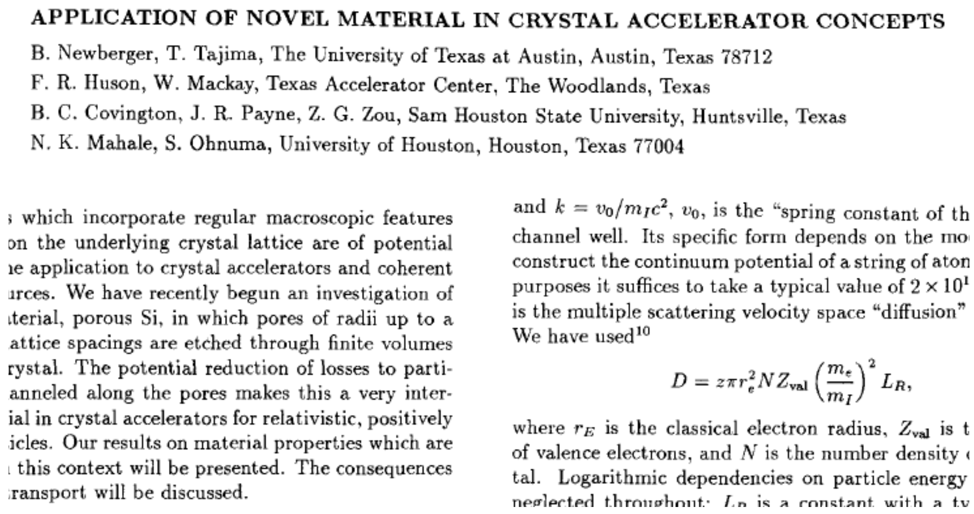

APPLICATION OF NOVEL MATERIAL IN CRYSTAL ACCELERATOR CONCEPTS

B. Newberger, T. Tajima, The University of Texas at Austin, Austin, Texas 78712
F. R. Huson, W. Mackay, Texas Accelerator Center, The Woodlands, Texas
B. C. Covington, J. R. Payne, Z. G. Zou, Sam Houston State University, Huntsville, Texas
N. K. Mahale, S. Ohnuma, University of Houston, Houston, Texas 77004

; which incorporate regular macroscopic features
on the underlying crystal lattice are of potential
ıe application to crystal accelerators and coherent
ırces. We have recently begun an investigation of
ıterial, porous Si, in which pores of radii up to a
attice spacings are etched through finite volumes
rystal. The potential reduction of losses to parti-
anneled along the pores makes this a very inter-
ial in crystal accelerators for relativistic, positively
icles. Our results on material properties which are
ı this context will be presented. The consequences
ransport will be discussed.

and $k = v_0/m_I c^2$, v_0, is the "spring constant of th
channel well. Its specific form depends on the mo
construct the continuum potential of a string of aton
purposes it suffices to take a typical value of 2×10^1
is the multiple scattering velocity space "diffusion"
We have used[10]

$$D = 2\pi r_e^2 N Z_{\rm val} \left(\frac{m_e}{m_I}\right)^2 L_R,$$

where r_E is the classical electron radius, $Z_{\rm val}$ is t
of valence electrons, and N is the number density
tal. Logarithmic dependencies on particle energy

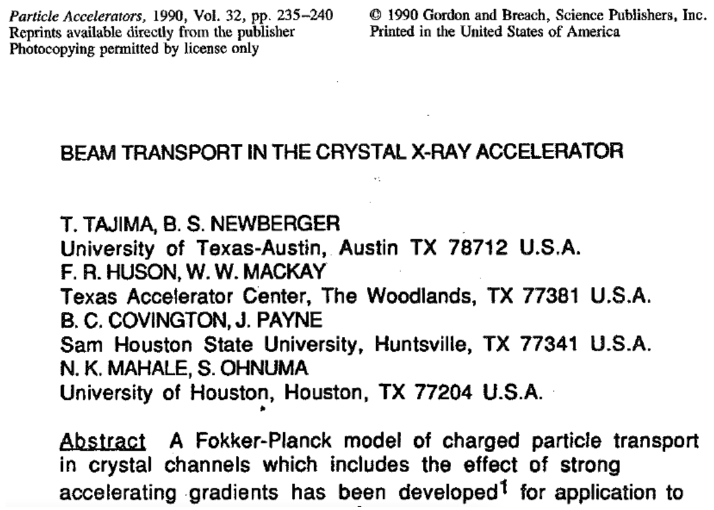

Particle Accelerators, 1990, Vol. 32, pp. 235–240
Reprints available directly from the publisher
Photocopying permitted by license only

BEAM TRANSPORT IN THE CRYSTAL X-RAY ACCELERATOR

T. TAJIMA, B. S. NEWBERGER
University of Texas-Austin, Austin TX 78712 U.S.A.
F. R. HUSON, W. W. MACKAY
Texas Accelerator Center, The Woodlands, TX 77381 U.S.A.
B. C. COVINGTON, J. PAYNE
Sam Houston State University, Huntsville, TX 77341 U.S.A.
N. K. MAHALE, S. OHNUMA
University of Houston, Houston, TX 77204 U.S.A.

Abstract A Fokker-Planck model of charged particle transport in crystal channels which includes the effect of strong accelerating gradients has been developed[1] for application to

VOLUME 59, NUMBER 13 PHYSICAL REVIEW LETTERS 28 SEPTEMBER 1987

Crystal X-Ray Accelerator

T. Tajima
Department of Physics and Institute for Fusion Studies, The University of Texas, Austin, Texas 78712
and
M. Cavenago
Department of Physics, University of California, Irvine, California 92717

(Received 18 November 1986)

An ultimate linac structure is realized by an appropriate crystal lattice (superlattice) that serves as a "soft" irised waveguide for x rays. High-energy ($\simeq$40 keV) x rays are injected into the crystal at the Bragg angle to cause Bormann anomalous transmission, yielding slow-wave accelerating fields. Particles (e.g., muons) are channeled along the crystal axis.

PACS numbers: 52.75.Di, 41.80.–y, 61.80.Mk

An approach to the attainment of ever higher energies by extrapolating the linac to higher accelerating fields, higher frequencies, and finer structures is prompted by several considerations, including the luminosity requirement which demands the radius of the colliding-beam spot be proportionately small at high energies: $a_0 = \pi^{-1/2}\hbar c(f\mathcal{N})^{-1/2}P\epsilon^{-2}$, where f, $\mathcal{N}$, P, and ϵ are the duty cycle, total number of events, beam power, and beam energy, respectively. This approach, however, encounters a physical barrier when the photon energy becomes of the order $\hbar\omega \simeq \hbar\omega_p \simeq mc^2\alpha^2 \simeq 30$ eV (α = the fine-structure constant), corresponding to wavelength (scale length) $\lambda \simeq 500$ Å: The metallic wall begins to absorb the photon strongly, where ω_p is the plasma frequency corresponding to the crystal electron density. In addition, since the wall becomes not perfectly conducting for $\hbar\omega \gtrsim mc^2\alpha^2$, the longitudinal component of fields becomes small and the photon goes almost straight into the wall (a soft-wall regime). As the photon energy $\hbar\omega$ much exceeds $mc^2\alpha^2$ and becomes $\gtrsim mc^2\alpha$, however, the metal now ceases to be opaque. The mean free path of the photon is given by Bethe-Bloch theory as $l_i = (3/2^8\pi) \times a_B^{-2}\alpha^{-1}n^{-1}(\hbar\omega/Z_{\rm eff}^2\mathcal{R})^{7/2}$, where a_B is the Bohr radius, n the electron density, $Z_{\rm eff}$ the effective charge of the lattice ion, and $\mathcal{R}$ the Rydberg energy.

In the present concept the photon energy is taken at the hard x-ray range of $\hbar\omega = mc^2\alpha$ and the linac structure is replaced by a crystal structure, e.g., silicon or GaAs-AlAs. (A similar bold endeavor was apparently undertaken by Hofstadter already in 1968.[1]) Here the crystal axis provides the channel through which accelerated particles propagate with minimum scattering (channeling[2]) and the x rays are transmitted via the Bormann effect (anomalous transmission[3,4]) when the x rays (wavelength λ) are injected in the xz plane with a

where b is the transverse lattice constant and later a the longitudinal lattice constant ($a \simeq b$) (see Fig. 1). The row of lattice ions (perhaps with inner-shell electrons) constitutes the "waveguide" wall for x rays, while they also act as periodic irises to generate slow waves. A superlattice[5] such as $\mathrm{Ge}_c\mathrm{Si}_{1-c}\mathrm{S}_l$ (in which the relative concentration c ranges from 0 to 1 over 100 Å or longer in the longitudinal z direction) brings in an additional freedom in the crystal structure and provides a small Brillouin wave number $k_s = 2\pi/s$ with s being the periodicity length. We demand that the x-ray light in the crystal channel walls becomes a slow wave and satisfies the high-energy acceleration condition

$$\omega/(k_z + k_s) = c, \tag{2}$$

where ω and k_z are the light frequency and longitudinal wave number.

The energy loss of moving particles in matter is due to ionization, bremsstrahlung, and nuclear collisions. We can show[6] that a channeled high-energy particle moving fast in the z direction oscillates in the xy plane according to the Hamiltonian

$$H = \frac{1}{2m}(p_x^2 + p_y^2) + V(x,y), \tag{3}$$

Porous Nanomaterial:

rastering possible

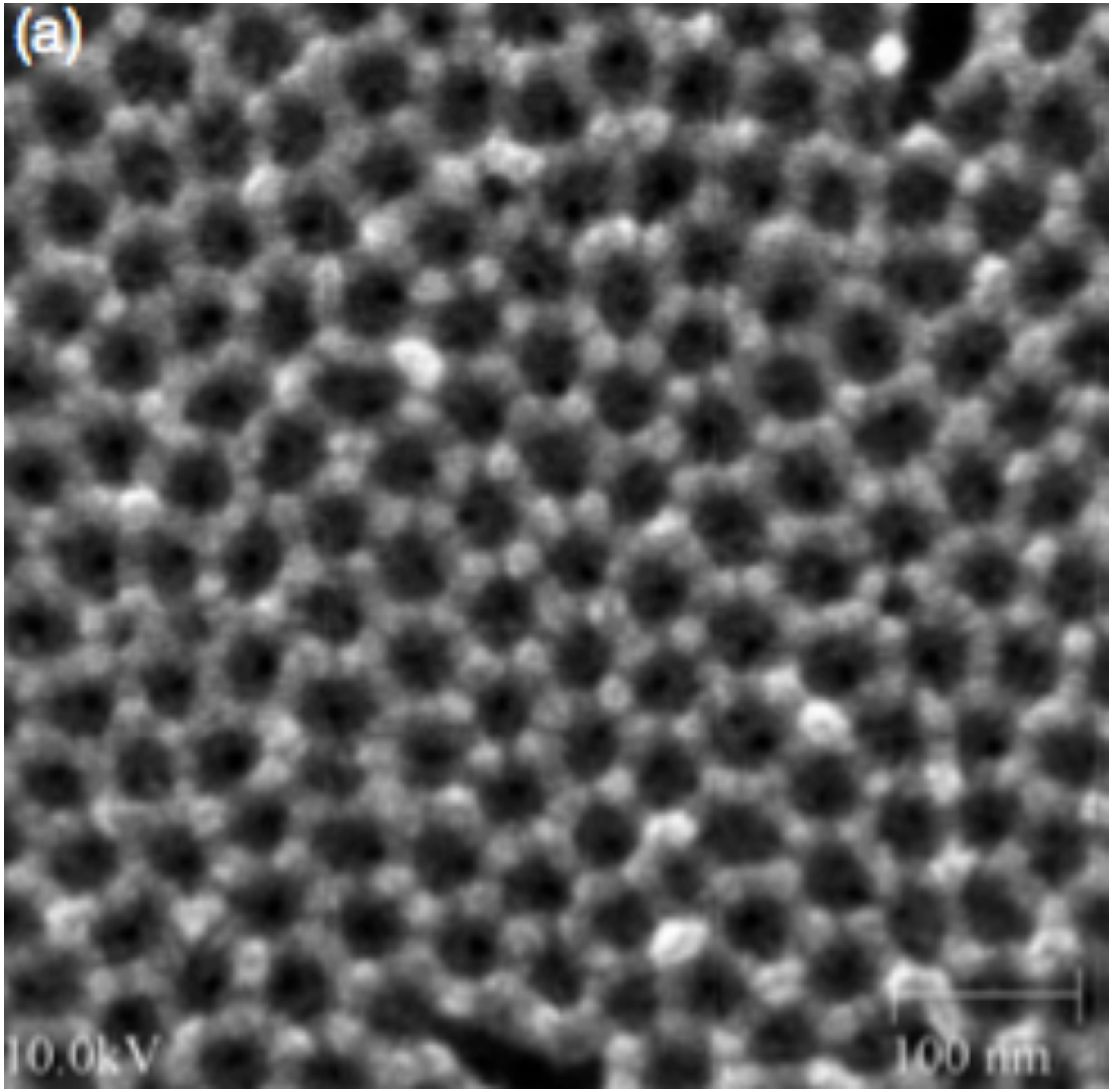

Nano holes:
reduce the stopping power
keep strong wakefields

➔ Marriage of *nanotech* and *high field science*

Spatia (nm), time(as-zs), density 10^{24} /cc), photon (keV) scales:
Transverse and longitudinal **structure of nanotubes**: act as e.g., accelerator structure (the structure intact in time of ionization, material breakdown times fs > x-ray pulse time zs-as)

Porous alimina on Si substrate
Nanotech. **15**, 833 (2004);
P. Taborek (UCI): porous alumina (2007)

UCI/Fermilab efforts on nanostructure wakefield acceleration

16th Advanced Accelerator Concept Workshop (AAC2014)

TeV/m Nano-Accelerator

Current Status of CNT-Channeling Acceleration Experiment

Y. M. Shin[1,2], A. H. Lumpkin[2], J. C. Thangaraj[2], R. M. Thurman-Keup[2], P. Piot[1,2], and V. Shiltsev[2]

Thanks to X. Zhu, D. Broemmelsiek, D. Crawford, D. Mihalcea, D. Still, K. Carlson, J. Santucci, J. Ruan, and E. Harms

[1]Northern Illinois Center for Accelerator and Detector Development (NICADD), Department of Physics, Northern Illinois University

[2]Fermi National Accelerator Laboratory (FNAL)

X-ray wakefield acceleration in nanomaterials tubes

T. Tajima, EPJ (2014)

X-ray laser with short length and small spot:

NB: electrons in outers-shell bound states, too, interact with X-rays

Simulation:

X.M. Zhang, et al.PR AB (2016)

Laser pulse with small spot can be well controlled and guided with a tube. Such structure available e.g. with **carbon nanotube,** or **alumina nanotubes** (typical simulation parameters)

$$\lambda = 1nm, a_0 = 4, \sigma_L = 5nm, \tau_L = 3nm / c$$

$$n_{tube} = 5 \times 10^{24} / cm^3, \sigma_{tube} = 2.5nm$$

Wakefield comparison between the cases of a tube and a uniform density

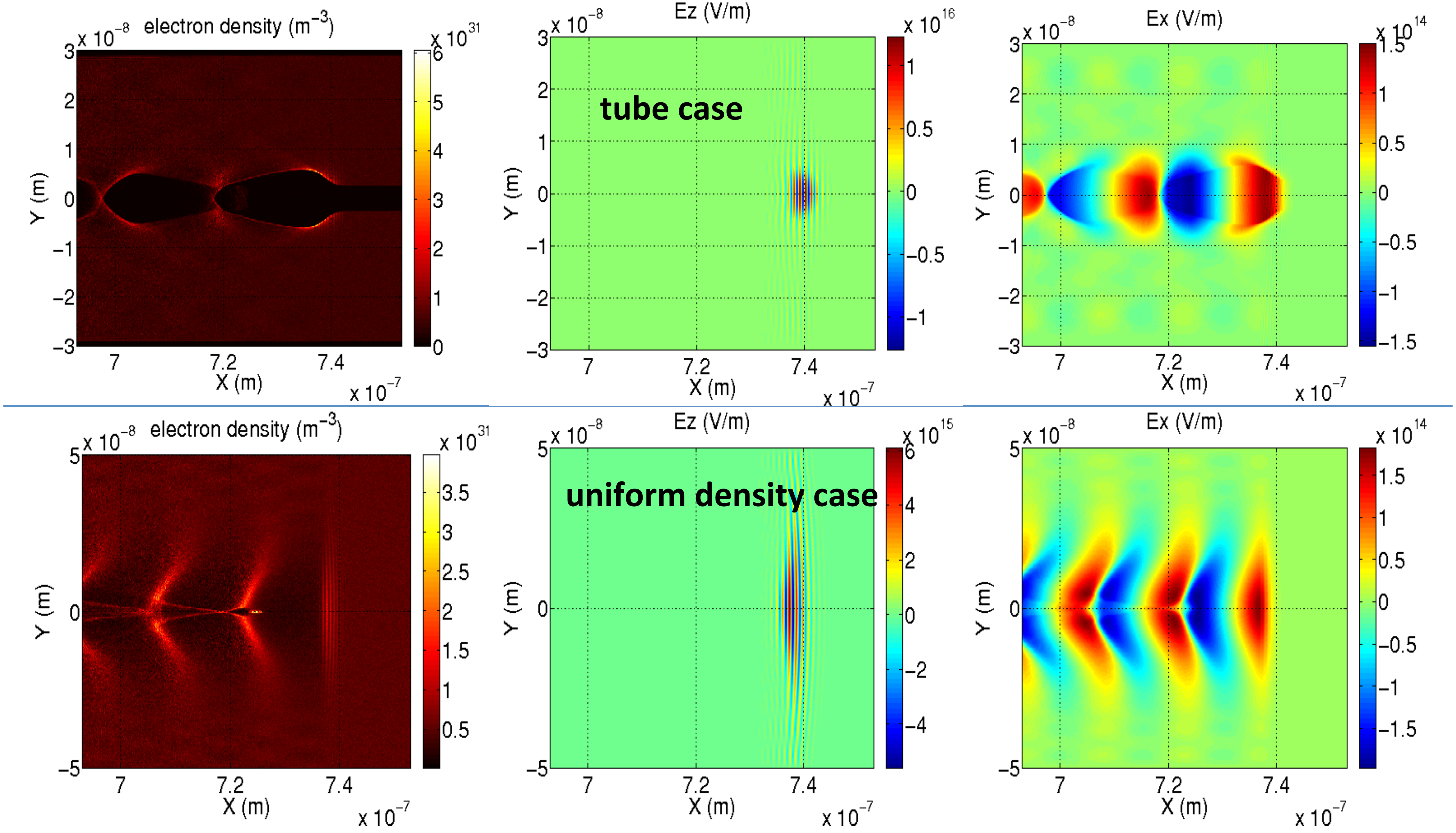

X. M. Zhang

PIC simulation of X-ray wakefields in a nanomaterial tube: Density scaling

Photon energy = 1keV,tube radius = 5nm, a_0=4, a few-cycled laser (around n_{cr} / n = 200)

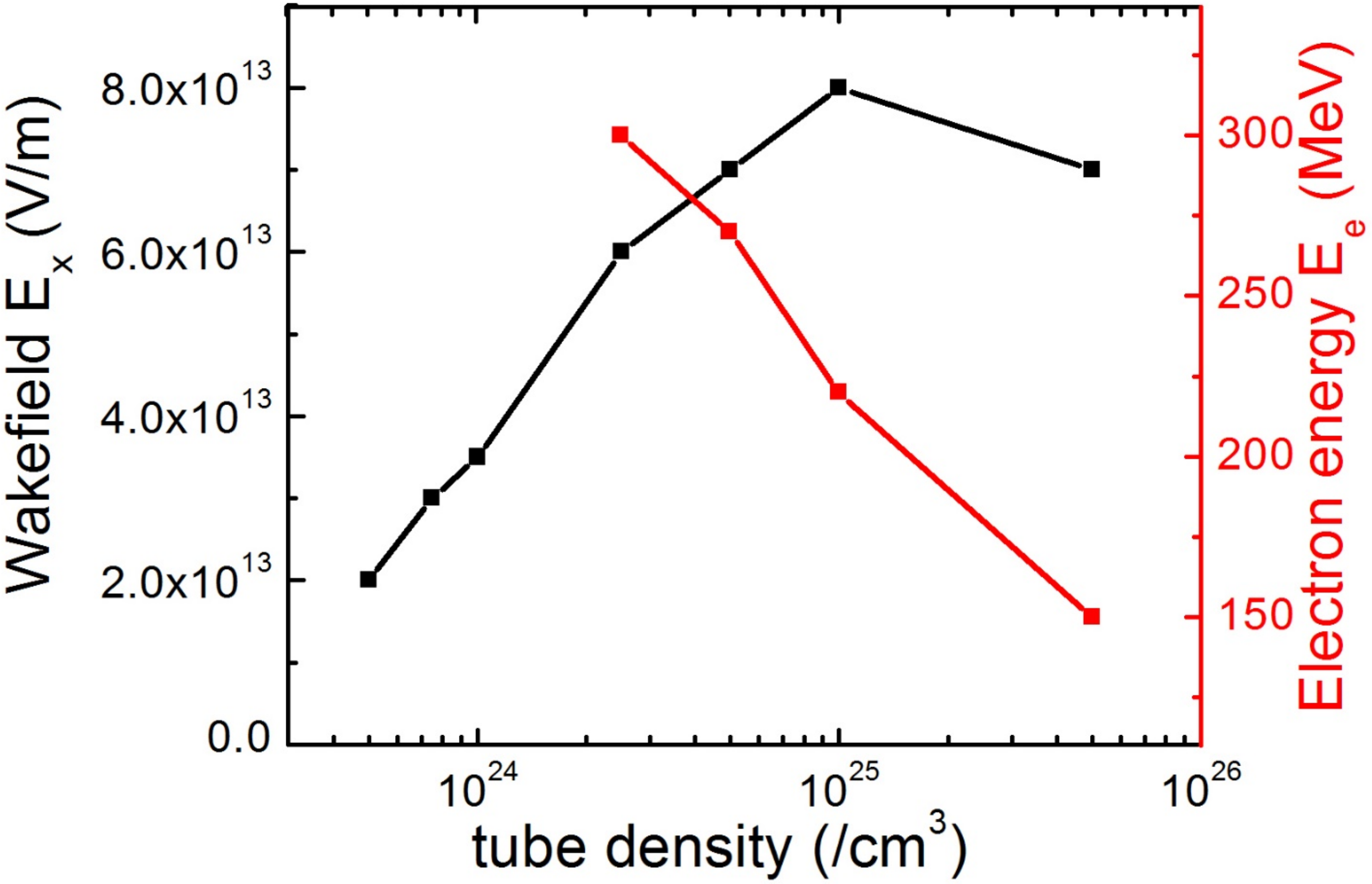

X. M. Zhnag (2016)

Wakefield scaling to the X-ray laser amplitude

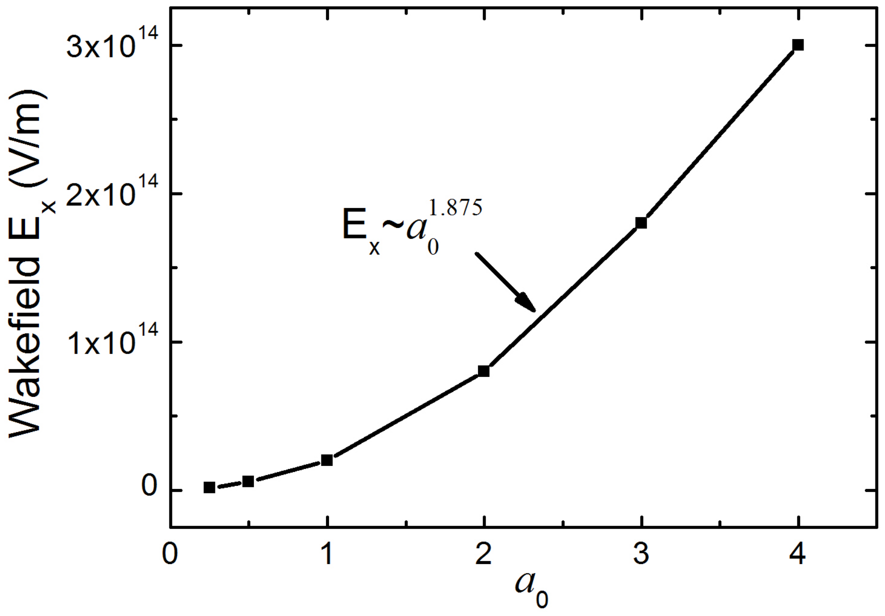

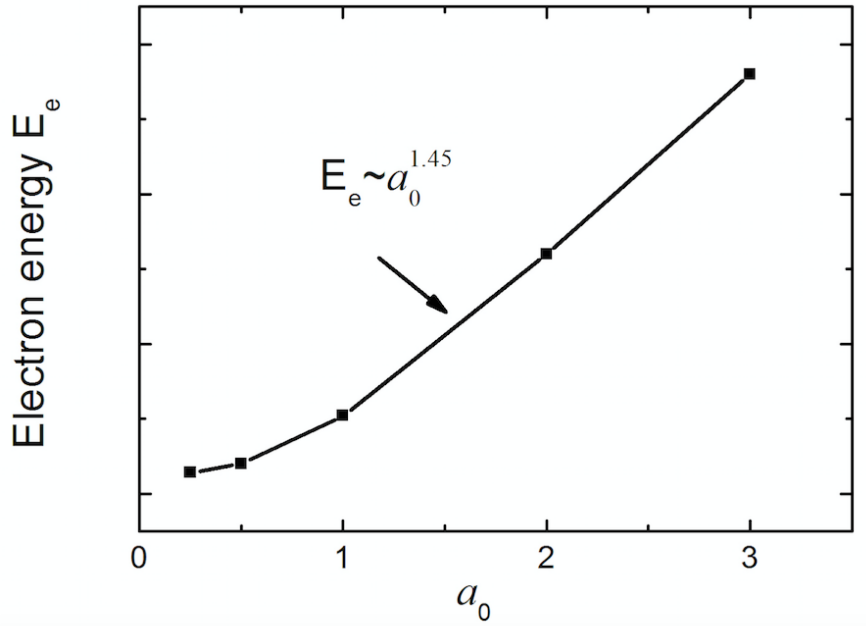

X. M. Zhnag (2016)

Wakefields and the tube geometry

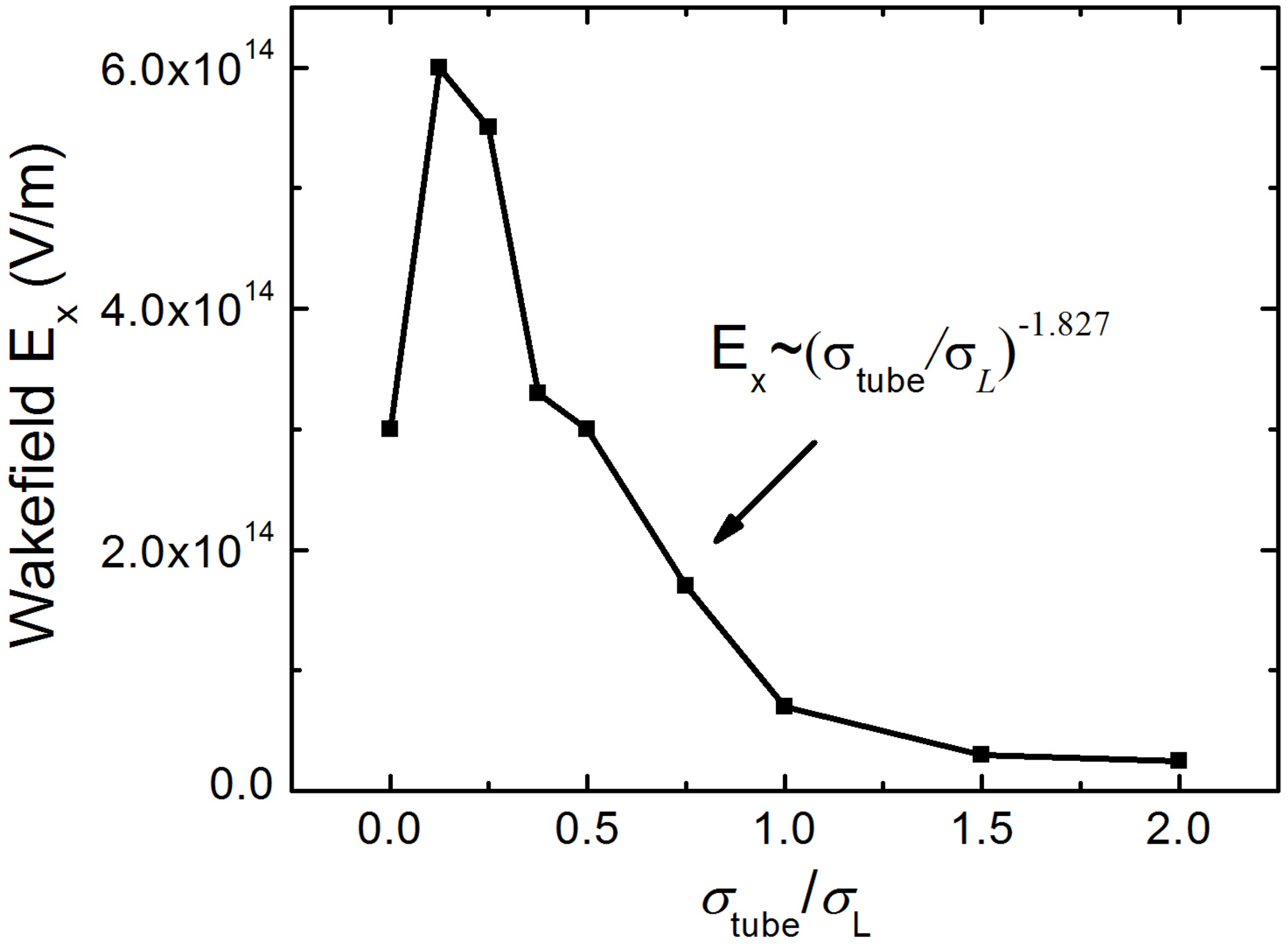

X. M. Zhang (2016)

With and without **optical phonon branch**

Model of optical phonon branch: *T. Tajima and S. Ushioda, PR B (1978)*

→ nanoplasmonics in X-ray regime

Without lattice force (i.e. plasma)

(when ω_{TO} is much smaller than ω_{pe}, there is no noticeable difference from the below where $\omega_{TO} = 0$)

With lattice force (optical phonon branch present)

$$\epsilon = 1 - \frac{\omega_{pe}^2}{\omega^2} - \frac{\Omega_p^2}{\omega^2 - \omega_{TO}^2}$$

$$\frac{\omega_{TO}}{\omega_{pe}} \simeq 0.75 \qquad \frac{\Omega_p}{\omega_{pe}} \simeq \frac{1}{43}$$

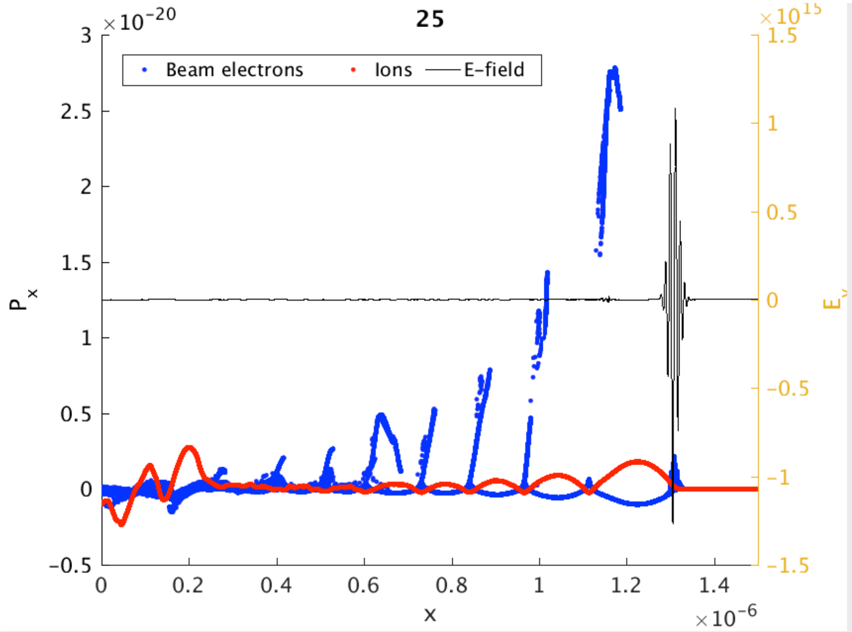

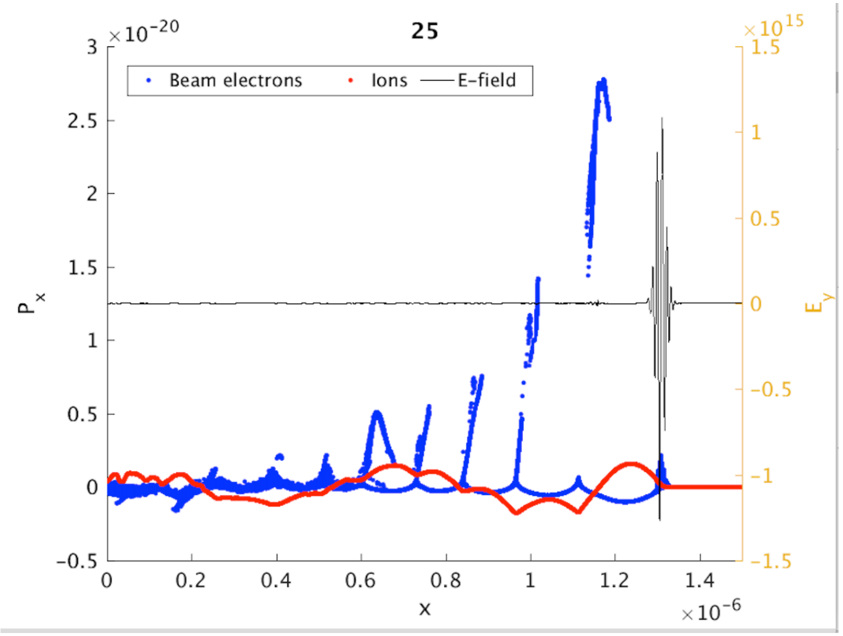

S. Hakimi, et al. (2017)

Wakefield **on a chip**

toward TeV over cm (beam-driven)

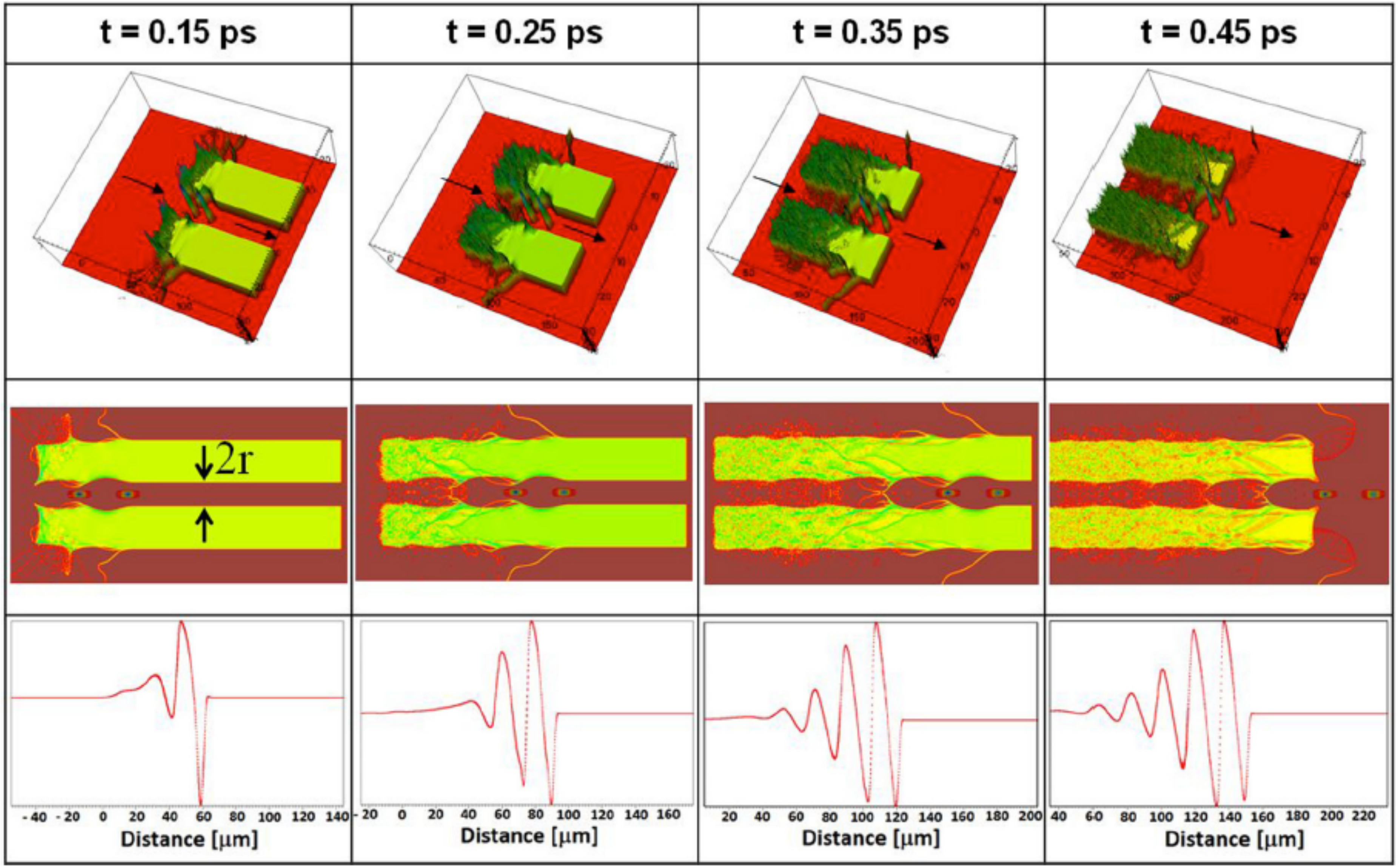

Y. Shin (2014)

Conclusions

- A new direction of ultrahigh intensity: **zeptosecond lasers**
- **EW 10keV X-rays laser** from 1PW optical laser
- Single-cycled optical laser → More efficient and more coherent acceleration of ions
- Single-cycled X-ray laser pulse (relativistic compression)
- **X-ray LWFA in crystal**: accelerating gradient 1-10TeV/cm, accelerating length 1-10m, energy gain per stage PeV; *mini-accelerators* (mm-m; portable) for GeV, TeV, PeV (and beyond)
- **Crystal nanoengineering**: s.a. nanoholes, arrays, focus nano-optics for nano-accelerator
- **Zeptosecond nano-beams** of *electrons*, *protons* (ions), muons, coherent γ-rays to very high energies: new tools for nuclear science
- PIC (w/QED) simulation shows support of the X-ray wakefields
- Start of zeptoscience: ELI-NP zeptoproject (collaboration)--- laser tools fit for nuclear phys. (←→attoseconds for atoms)
- **Scales revolution**: eV→keV; PW→EW; as→zs; μm→nm; GeV/cm→TeV/cm; 100m→cm; μ-beam→nanobeam; 10^{18} /cc → 10^{24}/cc

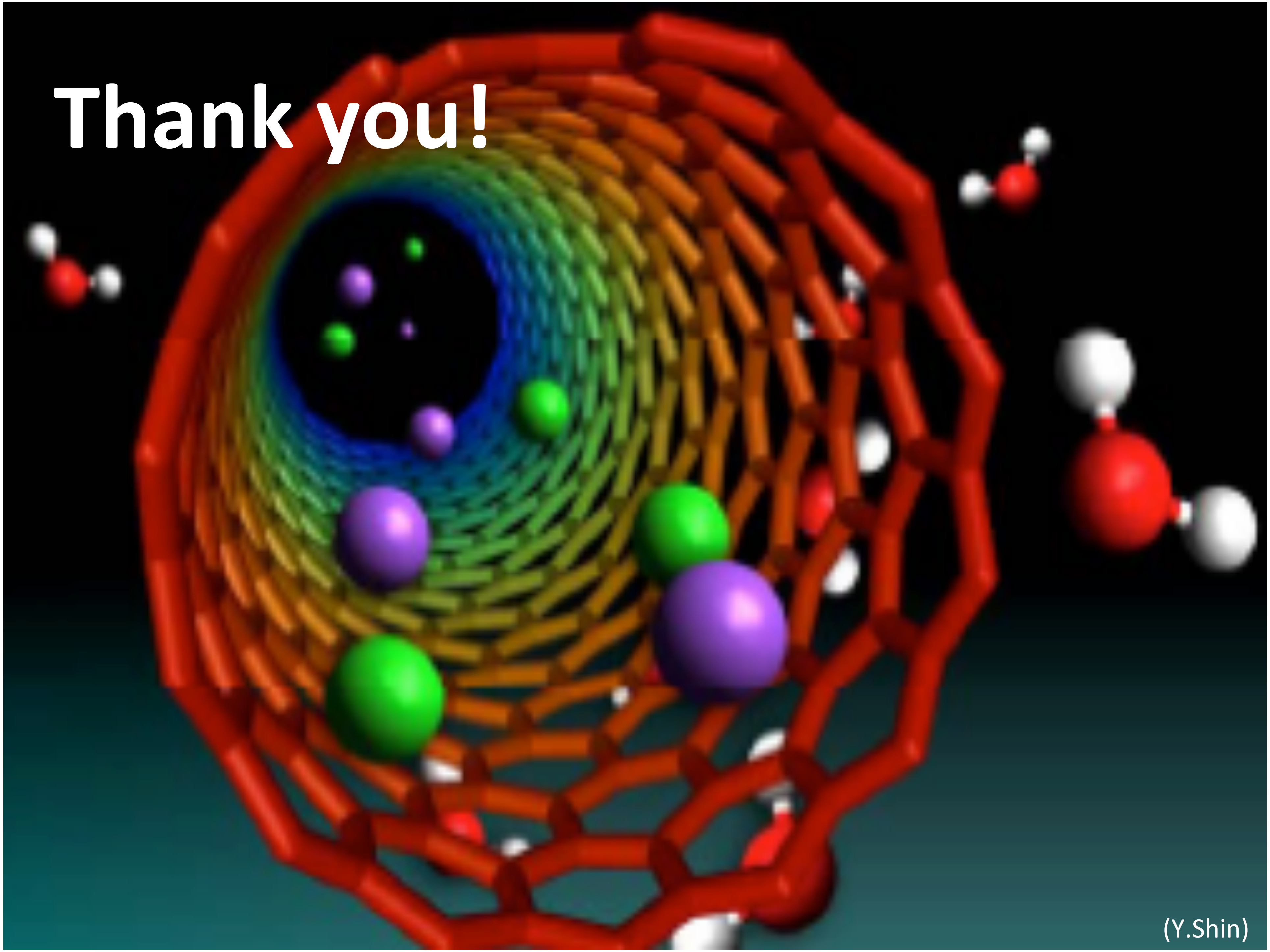

Thank you!

(Y.Shin)